Fractional-order nonsingular terminal sliding mode controller for a quadrotor with disturbances

M. Labbadi, A.J. Muñoz-Vázquez, Mohamed Djemai, Yassine Boukal, M. Zerrougui, M. Cherkaoui

Fractional-Order Nonsingular Terminal Sliding Mode Controller for a Quadrotor with disturbances

M. Labbadi[a], A. J. Muñoz-Vázquez[b], M. Djemai[a], Y. Boukal[c], M. Zerrougui[d], M. Cherkaoui[e]

[a] *LAMIH, CNRS, UMR-8201, INSA HdF UPHF, Valenciennes 59313, France*
[b] *College of Engineering, Texas A&M University, 6200 Tres Lagos Blvd, Higher Education Center at McAllen, Texas 78504, USA*
[c] *Aeronautics, Space & Defense division, ALTRAN, 4 Avenue Didier Daurat, 31700 Blagnac, France.*
[d] *University of Aix-Marseille, LIS UMR 7020 CNRS, 52 Av. Escadrille Normandie-Niemen 13397 Marseille, France*
[e] *Engineering for Smart and Sustainable Systems Research Center, Mohammadia School of Engineers, Mohammed V University in Rabat, Morocco*

Abstract

This paper proposes a finite-time controller for an unmanned aerial vehicle in the presence of disturbances/uncertainties using fractional-order terminal sliding mode. First, contrary to existing fractional-order backstepping sliding mode controllers, this paper introduces a new control approach for quadrotor position control, which is based on fractional-order fast terminal backstepping sliding mode control. Using an appropriate sliding surface, the position tracking error converges to zero in finite time while providing good robustness properties in different complex path scenarios under unknown disturbances. Then, a novel fractional-order fast terminal sliding mode control scheme is developed for quadrotor attitude control, which provides good properties in terms of robustness against unknown disturbances, and in terms of convergence time, etc. Finally, simulation results are presented to discuss the advantages of the hybrid control approach proposed in this work for quadrotors under unknown disturbances compared to other existing controllers.

Keywords: Quadrotor UAV, Backstepping, Terminal sliding mode control,

*Corresponding author
Email address: moussa.labbadi@uphf.fr (M. Labbadi[a])

Finite-time stabilization, Fractional-order control.

Nomenclature

Acronyms

QUAS	Quadrotor unmanned aerial system
TSMC	Terminal sliding mode control
SMC	Sliding mode control
FO	Fractional-order
PID	Proportional integral derivative
FOSM	Fractional-order sliding mode
FOHFTC	Fractional-order hybrid finite-time control
FOFTSMC	Fractional-order fast terminal sliding mode control
IBSMC	Integral backstepping sliding mode control
FOBSMC	Fractional-order backstepping sliding mode control
ISE	Integral square error
IADU	Integral of absolute value of the derivative of the input

Quadrotor parameters

$\begin{bmatrix} x(t) & y(t) & z(t) \end{bmatrix}^T$	Coordinates in the inertial frame
$\begin{bmatrix} \phi(t) & \theta(t) & \psi(t) \end{bmatrix}^T$	Roll, pitch, and yaw angles
$\begin{bmatrix} \mathbf{u}_F & \mathcal{M}_{xx} & \mathcal{M}_{yy} & \mathcal{M}_{zz} \end{bmatrix}^T$	Thrust and torques
$\begin{bmatrix} \mathbf{I}_1 & \mathbf{I}_2 & \mathbf{I}_3 \end{bmatrix}^T$	Inertial moments
$\begin{bmatrix} \mathcal{D}_x(t) & \mathcal{D}_y(t) & \mathcal{D}_z(t) \end{bmatrix}^T$	External disturbances in position loop
$\begin{bmatrix} \mathcal{D}_\phi(t) & \mathcal{D}_\theta(t) & \mathcal{D}_\psi(t) \end{bmatrix}^T$	External disturbances in attitude loop
$\begin{bmatrix} K_1 & K_2 & K_3 \end{bmatrix}^T$	Drag Coefficients for Rotational Motions
$\begin{bmatrix} K_4 & K_5 & K_6 \end{bmatrix}^T$	Drag Coefficients for Transitional Motions
$\begin{bmatrix} m & g \end{bmatrix}^T$	Mass and gravitational acceleration
$\begin{bmatrix} \hbar_b & \hbar_c \end{bmatrix}^T$	Thrust and drag factors
J_r and ω_i	Rotor inertia and speed of rotor i

Symbols

$e(t)$	Tracking error
$\mathcal{S}(t)$	Sliding manifold
D^q	Fractional order derivative
I^q	Fractional order integral
V	Lyapunov function
$\begin{bmatrix} x^r(t) & y^r(t) & z^r(t) \end{bmatrix}^T$	Desired position
$\begin{bmatrix} \phi^r(t) & \theta^r(t) & \psi^r(t) \end{bmatrix}^T$	Desired roll, pitch, and yaw angles
$\begin{bmatrix} v_x & v_y & v_z \end{bmatrix}^T$	Virtual signal controls
$\mathbf{t}_r$	finite time
$\lvert . \rvert$	Absolute value
q and α Fractional order operators	
β and γ	Positive coefficients
$\sigma, \varepsilon, K_{1i}$, and K_{1i}	Positive coefficients
h_{j1}, h_{j1}, and μ	Positive coefficients
c_i, k and c_j	Positive coefficients
δ	Positive function

1. Introduction

Advanced control techniques are implemented for quadrotor unmanned aerial systems (QUASs) to ensure a good path tracking such as hybrid controllers [1], fast nonsingular terminal sliding mode controllers [2, 3], backstepping terminal sliding mode controllers (TSMC) [4], aperiodic sampling based output feedback trajectory tracking controllers [5], finite-time reliable attitude tracking control [6], adaptive finite-time control [7], finite-time control [8], and state-dependent differential Riccati equation controllers [9], etc.

To provide good performance with respect to unknown wind gust disturbances and time-varying payloads, a robust adaptive prescribed performance

controller has been derived in [10]. The controller system was decoupled into position/attitude subsystems. A sliding mode control (SMC) with an adaptive law has been developed for translational subsystem while an adaptive backstepping technique has been designed to track the desired attitude. In [11], a finite-time control method was proposed for the quadrotor system under perturbations. It has been designed using a learning approach which consists in an adaptive neural control with a disturbance observer and a quaternion-based backstepping technique. The authors in [12] have proposed a combination of deterministic controllers and reinforcement learning for the safe flight of a micro quadrotor. In [13], an event-triggered control approach has been presented to reduce communication resources. The study in [14] has addressed the problems of actuator disturbance, time delay, and uncertainties/disturbances in attitude control for a quadrotor system. In this paper, a disturbance estimator-based attitude control law has been presented. A robust adaptive type-2 fuzzy neural controller optimized for quadrotor systems has been presented in [15].

A superior and innovative sliding surface should be carefully built with this goal in mind. It has been shown that fractional-order sliding mode is well-suite since fast response time and tiny overshoot can be accomplished at the same time, thanks to the memory effect in fractional calculus [16]. Many works on the control of engineering systems have been developed using fractional-order (FO) integral/derivative operators. To obtain good performances and a more flexible structure of proportioanl integral derivative (PID) controller, a fractional-order error manifold has been proposed in [17] for robot manipulators. In [18], the authors proposed to combine the concept of nonsingular terminal SMC and continuous FO dynamics for robot manipulators. The stabilization problem for Caputo-type FO systems under perturbation was addressed in [19] using a finite-time control based on sliding mode. A continuous fractional sliding mode control was proposed in [20] to deal with non-differentiable Hölder disturbances.

Moreover, various versions of fractional-order SMC have also been developed for QUAS in order to enhance performances and robustness against dis-

turbances [21]. In [22], the authors have combined the concept of backstepping technique and SMC with fractional order dynamics to provide good robustness properties of quadrotor systems for complex path under disturbances. In [23], a robust FOSM control technique has been proposed for attitude control and state constrained control approach has been designed for position control under Figures/uncertainties.

Motivated by the previous papers, and inspired by Refs. [22, 24], the current paper presents a FO hybrid finite-time control (FOHFTC) scheme with fractional order dynamics to deal with the trajectory tracking problem of quadrotor system. The disturbances and the variation of the drag coefficients of rotational and translational subsystems are considered in this study. The proposed FOHFTC is based on two loops. The first one is the position loop. It is based on a fractional order backstepping fast terminal SMC in order to obtain finite time stability of the position error. The second one is the attitude loop. It is based on a flexible FO fast terminal SMC. Besides, compared with the previous results, it can be seen that the proposed FOHFTC provides better performance such as fast response time, reduction of chattering phenomenon, rejection of Figures/uncertainties, etc. Compared to [22], where a classical fractional-order SMC was used, the current work presents a novel fractional-order terminal SMC for the outer-loop to track the desired position. Compared to [24], where a FOSMC was applied, the proposed approach is based on FO fast terminal SMC which increases the tracking performances. Furthermore, the FOHFTC proposed in this paper guarantees good disturbance rejection The contributions of the paper are highlighted as follows:

- Design of two new fractional order finite-time control strategies;
- Accurate tracking of a quadrotor with uncertainties and disturbances is obtained;
- The proposed control scheme ensures finite-time convergence of both the attitude and position velocity errors.

The paper is structured as follows; Section II presents the problem definition and formulation. Section III introduces the design of the proposed controller. Some simulation results are presented in Section IV. Finally, Section V provides the conclusion. **The notation $sig^a(y)$ represents $|y|^a sign(y)$.**

2. Problem definition and formulation

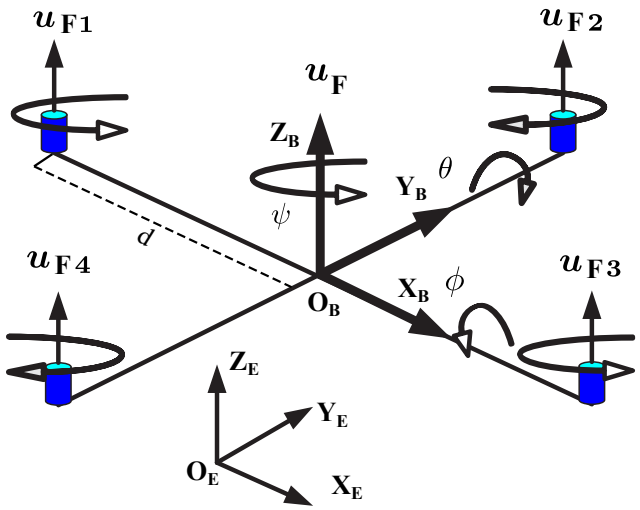

Figure 1: **Geometry of a QUAS.**

The orientation and position of quadrotor are modeled as a rigid body, described in the body frame O_B. The QUAS geometry shown in Fig. 1 is used to develop its dynamic model. This model is obtained by using the orthogonal rotation matrix $\mathcal{R}_\mathcal{T}$ which can be parametrized by the roll $\phi(t)$, pitch $\theta(t)$, and yaw $\psi(t)$ Euler angles in the Earth inertial frame E. $x(t)$, $y(t)$, and $z(t)$ are used to define the QUAS position in the O_E frame. The quadrotor dynamics are given as:

Table 1: Quadrotor Modelling.

Attitude dynamics	$\mathbf{I}\dot{\Omega} = -\Omega^T \times \mathbf{I}\Omega + \mathcal{M} + \mathcal{M}^a + \mathcal{M}^c + \mathcal{D}_\Omega(t)$
Position dynamics	$\mathbf{m}\ddot{\mathcal{P}} = \mathcal{R}_\mathcal{T}\mathbf{u}_F + \mathcal{T}^d + \mathcal{T}^g + \mathcal{D}_\mathcal{P}(t)$
Aerodynamic friction torque	$\mathcal{M}^a = diag\begin{bmatrix}-K_1\dot{\phi}^2(t) & -K_2\dot{\theta}^2(t) & -K_3\dot{\psi}^2(t)\end{bmatrix}^T$
Gyroscopic effects	$\mathcal{M}^c = -\sum_{i=1}^{i=4}\Omega^T J_r\begin{bmatrix}0 & 0 & (-1)^{i+1}\omega_i\end{bmatrix}^T$
Aerodynamic friction force	$\mathcal{T}^d = diag\begin{bmatrix}K_4\dot{x}(t) & -K_5\dot{y}(t) & -K_6\dot{z}(t)\end{bmatrix}^T$
Gravity force	$\mathcal{T}^g = \begin{bmatrix}0 & 0 & -g\end{bmatrix}^T$

One can defined the link between the angular velocities and control laws as:

$$\begin{bmatrix}\mathbf{u}_F\\ \mathcal{M}_{xx}\\ \mathcal{M}_{yy}\\ \mathcal{M}_{zz}\end{bmatrix} = \begin{bmatrix}\hbar_b & \hbar_b & \hbar_b & \hbar_b\\ 0 & \hbar_b & 0 & -\hbar_b\\ -\hbar_b & 0 & \hbar_b & 0\\ -\hbar_c & \hbar_c & -\hbar_c & \hbar_c\end{bmatrix}\begin{bmatrix}\omega_1^2\\ \omega_2^2\\ \omega_3^2\\ \omega_4^2\end{bmatrix} \tag{1}$$

The position subsystem of the QUAS is underacted with one input and three outputs. Three virtual control signals are designed to tackle this issue:

$$v = \begin{bmatrix}v_x\\ v_y\\ v_z\end{bmatrix} = \begin{bmatrix}(\sin\theta(t)\cos\phi(t)\cos\psi(t) + \sin\phi(t)\sin\psi(t))\frac{\mathbf{u}_F}{\mathbf{m}}\\ (\sin\theta(t)\cos\phi(t)\sin\psi(t) - \sin\phi(t)\cos\psi(t))\frac{\mathbf{u}_F}{\mathbf{m}}\\ (-g + \frac{1}{m}(\cos\theta(t)\cos\phi(t)\frac{\mathbf{u}_F}{\mathbf{m}}))\end{bmatrix} \tag{2}$$

Thus, the left thrust, and desired tilting angles can be defined using these virtual controls as:

$$\phi^r(t) = \arctan\left(\cos\theta^r(t)\frac{\sin\psi^r(t)v_x - \cos\psi^r(t)v_y}{v_z + g}\right) \tag{3a}$$

$$\theta^r(t) = \arctan\left(\frac{\cos\psi^r(t)v_x + \sin\psi^r(t)v_y}{v_z + g}\right) \tag{3b}$$

$$\mathbf{u}_F = \mathbf{m}\sqrt{v_x^2 + v_y^2 + (v_z + g)^2} \tag{3c}$$

The acontrol objective is to design the torque $\mathcal{M}$ and virtual signal controls to guarantee tracking of the desired trajectories:
$\begin{bmatrix}x^r(t) & y^r(t) & z^r(t) & \phi^r(t) & \theta^r(t) & \psi^r(t)\end{bmatrix}^T$.

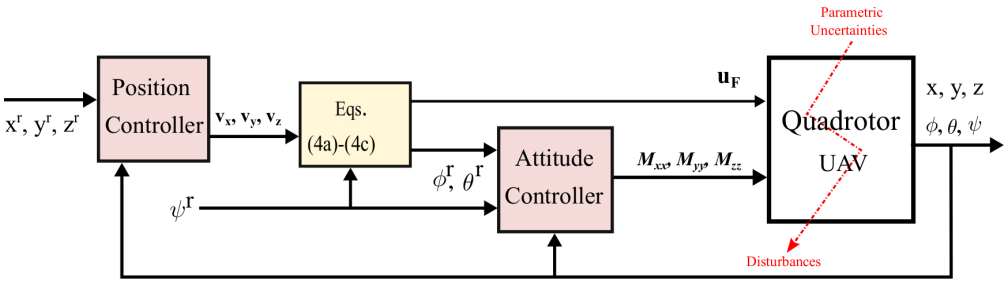

Figure 2: The proposed control scheme for QUAV.

3. Controller Design

The control structure of the QUAS in this paper is divided into an outer-loop (position loop), and an inner-loop (attitude loop), which includes the roll, pitch, and yaw angles. In this section, two nonlinear controllers are designed for the QUAS system. The first controller is a FO backstepping fast terminal sliding mode control, while the second one is a FO fast terminal SMC for the inner-loop.

3.1. Position Controller

In the following, the virtual control signals v_x, v_y will be designed. Let us first consider the altitude dynamics which can be considered as:

$$\begin{cases} \dot{\mathcal{Z}}_1(t) &= \mathcal{Z}_2(t) \\ \dot{\mathcal{Z}}_2(t) &= v_z - \frac{K_6}{m}\dot{\mathcal{Z}}_1(t) - g + \mathcal{D}_z(t) \end{cases} \tag{4}$$

where $\mathcal{Z}_1(t) = z(t)$ and $\mathcal{Z}_2(t) = \dot{z}(t)$ represent the state variable of altitude subsystem.

Define the tracking error of the altitude as:

$$e_z(t) = \mathcal{Z}_1(t) - z^r(t) \tag{5}$$

The derivative of $e_z(t)$ is

$$\dot{e}_z(t) = \dot{\mathcal{Z}}_1(t) - \dot{z}^r(t) \tag{6}$$

Define the Lyapunov function and its derivative as:

$$V_{z1}(t) = \frac{1}{2}e_z^2(t), \qquad \dot{V}_{z1}(t) = \dot{e}_z(t)e_z(t) \tag{7}$$

The derivative of $V_{z1}(t)$ can be rewritten as:

$$\dot{V}_{z1}(t) = \dot{e}_z(t)e_z(t) = e_z(t)(\mathcal{Z}_2(t) - \dot{z}^r(t)) \tag{8}$$

Let us set the following virtual control input $\mathcal{Z}_2^r$ as $e_{zz}(t) = \dot{\mathcal{Z}}_1 - \mathcal{Z}_2^r$.

Differentiating $V_{z1}(t)$, one gets,

$$\dot{V}_{z1}(t) = e_z(t)(\mathcal{Z}_2(t) - \dot{z}^r(t)) \tag{9}$$

$$= e_z(t)(e_{zz}(t) + \mathcal{Z}_2^r(t) - \dot{z}^r(t)) \tag{10}$$

The virtual input can be defined as: $\mathcal{Z}_2^r(t) = \dot{z}^r(t) - c_1 e_z(t)$ where c_1 is a positive constant. So, using this virtual input $\mathcal{Z}_2^r$, one obtains,

$$\dot{V}_{z1}(t) = e_z(t)e_{zz}(t) + e_z(t)(\mathcal{Z}_1^r - c_1 e_z(t) - \mathcal{Z}_1^r) \tag{11}$$

$$= e_z(t)e_{zz}(t) - c_1 e_z^2(t) \tag{12}$$

To consider the term $e_z(t)e_{zz}(t)$, a nonlinear sliding manifold is defined as:

$$\mathcal{S}_z(t) = e_z(t) + k_z e_{zz}(t) + sig(e_z(t))^{\mu_z} \tag{13}$$

with $k_z > 0$.

The equivalent law can be designed as:

$$v_{ze} = -(c_1 + k_z)\dot{e}_z(t) + g + \frac{K_6}{m}\dot{\mathcal{Z}}_1(t) + \ddot{\mathcal{Z}}^r(t) \tag{14}$$

To achieve robustness against $\mathcal{D}_z(t)$, a fractional-order switching law is designed as:

$$v_{zs} = -h_{z1}\mathcal{S}_z(t) - h_{z2}D^{q_z} sign(\mathcal{S}_z(t)) \tag{15}$$

where $h_{z1}, h_{z2} > 0$ and $q_z \in]0, 1[$. The term D^{q_z} represents FO derivative, which q_z is the fractional operator.

Remark 1. *Discontinuity at the origin prevents the differentiation of* $sign(\mathcal{S}_z(t))$, *It is replaced by* $\tanh(k\mathcal{S}_z(t))$ *function with* $k > 0$.

The ultimate altitude control is given by:

$$v_z = v_{zz} + v_{zs} \tag{16}$$

Assumption 1. ***The disturbances*** $\mathcal{D}_\Omega(t)$ ***and*** $\mathcal{D}_\mathcal{P}(t)$ ***represent the disturbances and uncertainties parameters of quadrotor, such as aerodynamic coefficients, mass, moments of inertia and the external factors. There exists*** $\gamma > 0$ ***such that*** $\mathcal{D}_i(t)$ ***is satisfied with*** $|\mathcal{D}_i| \leq \gamma |D^q \tanh(k\mathcal{S}_i(t))|$***. According to Lemma 1, one get*** $|\mathcal{D}_i| \leq \gamma$ ***with*** γ ***is a positive but unknown constant. We assumed that the perturbations affecting the quadcopter system are bounded.***

Lemma 1. ***[25] Consider the l derivative of the*** $\varphi(t)$
$D^q\varphi(t) = \frac{1}{\Gamma(1-q)} \frac{d}{dt} \int_0^t \frac{\varphi(\tau)}{(t-\tau)^q} d\tau,\ 0 \leqslant q < 1$***, the following inequalities are obtained***

$$D^q sign(\mathcal{S}_i(t)) = \begin{cases} > 0, & if\ \mathcal{S}_i(t) > 0,\ t > 0 \\ < 0, & if\ \mathcal{S}_i(t) < 0,\ t > 0 \end{cases} \tag{17}$$

where $\Gamma(.)$ ***is the Gamma function.***

Remark 2. ***Consider the following two cases: : (i)*** $\mathcal{S}(t) > 0\ \forall t > 0$***, we have*** $0 < D^q sgn(k\mathcal{S}_i(t)) < \frac{t^{-q}}{\Gamma(1-q)}$***; (ii)*** $\mathcal{S}(t) < 0\ \forall t > 0$***, one has*** $-\frac{t^{-q}}{\Gamma(1-q)} < D^q sgn(k\mathcal{S}_i(t)) < 0$***. Then,*** $D^q sgn(k\mathcal{S}_i(t))$ ***is bounded in both cases. Because the above situations have a higher absolute value than the others,*** $D^q sgn(k\mathcal{S}_i(t))\ \forall \mathcal{S}_i(t)$ ***is bounded, i.e. there exists*** $\varsigma > 0$ ***such that*** $|D^q sgn(k\mathcal{S}_i(t))| < \varsigma$***. On the other hand, due to the onboard power's restriction, the variation in the quadrotor flight states' attitude and trajectory subsystems cannot vary at a supernormal pace. There is also an upper limit to the amount of disturbances since turbulence***

and gusts, which make up the environment, are energy restricted and cannot last for a long period.

Theorem 1. *The origin of* ***position system presented in Table 1****, using Assumption 1 under the FO backstepping fast terminal sliding mode control designed in* (16) *and the nonlinear sliding variable* $\mathcal{S}_z(t)$*, is finite-time stable.*

Proof. Let us consider the Lyapunov function candidate

$$V_{z2}(t) = V_{z1}(t) + \frac{1}{2}\mathcal{S}_z^2(t) \tag{18}$$

Differentiating $V_{z2}(t)$ yields

$$\begin{aligned}\dot{V}_{z2}(t) = &-c_1 e_z^2(t) + e_z(t)e_{zz}(t) + \mathcal{S}_z(t)[(k_z + c_1)\dot{e}_z(t) - g \\ &+ v_z - \ddot{\mathcal{Z}}^r + \mathcal{D}_z(t)]\end{aligned} \tag{19}$$

According to Assumption 1 and replacing (16) into (19), one has

$$\begin{aligned}\dot{V}_{z2}(t) &= -c_1 e_z^2(t) + e_z(t)e_{zz}(t) - h_{z1}\mathcal{S}_z^2(t) \\ &\quad - h_{z2}\mathcal{S}_z(t)D^{q_z}\tanh(k_z\mathcal{S}_z(t)) + \mathcal{S}_z(t)\mathcal{D}_z(t) \\ &\leq -c_1 e_z^2(t) + e_z(t)e_{zz}(t) - h_{z1}\mathcal{S}_z^2(t) \\ &\quad - h_{z2}\mathcal{S}_z(t)D^{q_z}\tanh(k_z\mathcal{S}_z(t)) + \mathcal{S}_z(t)d_z \\ &\leq -c_1 e_z^2(t) + e_z(t)e_{zz}(t) - h_{z1}\mathcal{S}_z^2(t)\end{aligned} \tag{20}$$

One can define the following matrix in order to analyze the stability :

$$Q_\phi = \begin{bmatrix} c_1 + h_{z1}k_z^2 h_{z1}k_z & -0.5 \\ h_{z1}k_z & h_{z1} \end{bmatrix}, \quad \mathcal{E}_1 = \begin{bmatrix} e_z(t) \\ e_{zz}(t) \end{bmatrix} \tag{21}$$

If the Q_ϕ is positive matrix, then the derivative of the Lyapunov can be rewritten,

$$\dot{V}_{z2}(t) \leq -\mathcal{E}_1^T Q_\phi \mathcal{E}_1 \leq 0 \tag{22}$$

In order to explicate the expression of the reaching time, the switching controller can be defined in the integer order form as: $v_{zs} = -h_{z1}\mathcal{S}_z(t) - h_{z2}sign(\mathcal{S}_z(t))$. Thus, we could obtain $\mathcal{S}_z(t)\dot{\mathcal{S}}_z(t) = -h_{z1}\mathcal{S}_z^2(t) - h_{z2}|\mathcal{S}_z(t)|$. There are two scenarios based on the initial condition of $\mathcal{S}_z(0)$.

- Case 1: $\mathcal{S}_z(0) > 0$, one has $\dot{\mathcal{S}}_z(t)) = -h_{z1}\mathcal{S}_z(t) - h_{z2}$. The analytical solution is $\mathcal{S}_z(t)\left(\mathcal{S}_z(0) + \frac{h_{z2}}{h_{z1}}\right)e^{-h_{z1}t} - \frac{h_{z2}}{h_{z1}}$, then the reaching-time is $t_{rz} = \frac{1}{h_{z2}}ln\frac{h_{z2}\mathcal{S}_z(0)+h_{z1}}{h_{z1}} > 0$;

- Case 2: $\mathcal{S}_z(0) \leq 0$, one has $\dot{\mathcal{S}}_z(t)) = -h_{z1}\mathcal{S}_z(t) + h_{z2}$. The analytical solution is $\mathcal{S}_z(t)\left(-\mathcal{S}_z(0) + \frac{h_{z2}}{h_{z1}}\right)e^{-h_{z1}t} + \frac{h_{z2}}{h_{z1}}$, then the reaching-time is $t_{rz} = \frac{1}{h_{z2}}ln\frac{-h_{z2}\mathcal{S}_z(0)+h_{z1}}{h_{z1}} > 0$

From the two cases, the reaching time can be defined as $t_{rz} = \frac{1}{h_{z2}}ln\frac{h_{z2}|\mathcal{S}_z(0)|+h_{z1}}{h_{z1}} > 0$. Simultaneously, the reaching time of the switching FO controller $v_{zs} = -h_{z1}\mathcal{S}_z(t) - h_{z2}D^{q_z}sign(\mathcal{S}_z(t))$ can be defined by two cases.

- Case 3: $\mathcal{S}_z(0) > 0$, one has $\dot{\mathcal{S}}_z(t) = -h_{z1}\mathcal{S}_z(t) - h_{z2}D^{q_z}sign(\mathcal{S}_z(t))$. Therefore, one obtain $\left(\mathcal{S}_z(t)e^{h_{z2}t}\right)' = e^{h_{z2}t}(\dot{\mathcal{S}}_z(t) + h_{z2}\mathcal{S}_z(t))$. Therefore, $\mathcal{S}_z(t)e^{h_{z2}t} = \mathcal{S}_z(0) - \frac{h_{z1}}{\Gamma(1-q_z)}\int_0^t \tau^{-q_z}e^{h_{z2}\tau}d\tau$. Also, we can handle $\mathcal{S}_z(t_{reach})e^{h_{z2}t} = \mathcal{S}_z(0) - \frac{h_{z1}}{\Gamma(1-q_z)}\int_0^{t_{reach}} \tau^{-q_z}e^{h_{z2}\tau}d\tau = \frac{\mathcal{S}_z(0)\Gamma(1-q_z)}{h_{z1}} = 0$, since $\mathcal{S}_z(t_{reach}) = 0$. Hence, the settlement of $\mathcal{S}_z(0) = \frac{h_{z1}}{\Gamma(1-q_z)}\int_0^t \tau^{-q_z}e^{h_{z2}\tau}d\tau$ is t_{reach}. Let, $\Upsilon(t) = \int_0^t \tau^{-q_z}e^{h_{z2}\tau}d\tau = \frac{\mathcal{S}_z(0)\Gamma(1-q_z)}{h_{z1}} > 0$. Clearly, $\Upsilon(t), t \in [0, \inf)$ is an increasing function. According to intermediate value theorem, there exists t^* such that $\Lambda(t^*) = \frac{\mathcal{S}_z(0)\Gamma(1-q_z)}{h_{z1}}$. Applying numerical approximation, we can gain $t_{reach} = t^*$.

- Case 4 : $\mathcal{S}_z(0) < 0$, we can have $\dot{\mathcal{S}}_z(t) = -h_{z1}\mathcal{S}_z(t) - h_{z2}D^{q_z}sign(\mathcal{S}_z(t))$. One obtain $\left(\mathcal{S}_z(t)e^{h_{z2}t}\right)' = e^{h_{z2}t}(\dot{\mathcal{S}}_z(t) + h_{z2}\mathcal{S}_z(t)) = \frac{h_{z1}}{\Gamma(1-q_z)}t^{-q_z}e^{h_{z2}t}$. We can handle $\mathcal{S}_z(t_{reach})e^{h_{z2}t} = \mathcal{S}_z(0) + \frac{h_{z1}}{\Gamma(1-q_z)}\int_0^{t_{reach}} \tau^{-q_z}e^{h_{z2}\tau}d\tau = \frac{\mathcal{S}_z(0)\Gamma(1-q_z)}{h_{z1}} = 0$. Let, $\Upsilon(t) = \int_0^t \tau^{-q_z}e^{h_{z2}\tau}d\tau = \frac{\mathcal{S}_z(0)\Gamma(1-q_z)}{h_{z1}} > 0$. Similar to case 3, there exists $t^* > 0$ such that $\Lambda(t^*) = \frac{-\mathcal{S}_z(0)\Gamma(1-q_z)}{h_{z1}}$. Applying numerical approximation, we can gain $t_{reach} = t^*$. Therefore, t_{teach} of

FO switching controller can be obtained from $\Upsilon(t) = \int_0^t \tau^{-q_z} e^{h_{z2}\tau} d\tau = \frac{\mathcal{S}_z(0)\Gamma(1-q_z)}{h_{z1}}$.

□

Similar to v_z, one can defined the following two controllers. For the $y(t)$ channel:

$$\begin{aligned} v_y &= v_{ye} + v_{ys} \\ &= -h_{y1}\mathcal{S}_y(t) - h_{y2}D^{q_y} sign(\mathcal{S}_y(t)) - (c_2 + k_y)\dot{e}_y(t) + \frac{K_5}{m}\dot{\mathcal{Y}}_1(t) + \ddot{\mathcal{Y}}^r(t) \end{aligned} \tag{23}$$

and

$$\begin{aligned} v_x &= v_{xe} + v_{xs} \\ &= -h_{x1}\mathcal{S}_x(t) - h_{x2}D^{q_x} sign(\mathcal{S}_x(t)) - (c_3 + k_x)\dot{e}_x(t) + \frac{K_4}{m}\dot{\mathcal{X}}_1(t) + \ddot{\mathcal{X}}^r(t) \end{aligned} \tag{24}$$

where $h_{x1}, h_{x2} > 0$, $q_x, q_y \in]0,1[^2$ $c_1, c_2 > 0$ and $h_{y1}, h_{y2} > 0$. $\mathcal{X}_1(t)$ and $\mathcal{X}_2(t) = \dot{\mathcal{X}}_1(t)$ represent the state variable of $x(t)-$subsystem. The notations $\mathcal{Y}_1(t)$ and $\mathcal{Y}_2(t) = \dot{\mathcal{Y}}_1(t)$ represent the state variable of $y(t)-$subsystem.

Theorem 2. *The origin of* ***position system presented in Table 1****, using Assumprion 1 under the FO backstepping fast terminal sliding mode controls designed in* (16)**,** (23)**,** (24) *and the nonlinear sliding variable the nonlinear sliding variables* $\mathcal{S}_x(t), \mathcal{S}_y(t)$*, and* $\mathcal{S}_z(t)$*, is finite-time stable.*

Proof. The Lyapunov function for the position subsystem can be used as follows:

$$\begin{aligned} V_T &= V_{z2}(t) + V_{x2}(t) + V_{y2}(t) \\ &= V_{z1}(t) + \frac{1}{2}\mathcal{S}_z^2(t) + V_{x1}(t) + \frac{1}{2}\mathcal{S}_x^2(t) + V_{y1}(t) + \frac{1}{2}\mathcal{S}_y^2(t) \end{aligned} \tag{25}$$

The derivative of V_T is,

$$\begin{aligned} \dot{V}_T = &-c_1 e_z^2(t) + e_z(t)e_{zz}(t) + \mathcal{S}_z(t)[(k_z + c_1)\dot{e}_z(t) - g \\ &+ v_z - \ddot{\mathcal{Z}}^r + \mathcal{D}_z(t)] \\ &- c_3 e_x^2(t) + e_x(t)e_{xx}(t) + \mathcal{S}_x(t)[(k_x + c_3)\dot{e}_x(t) \\ &+ v_x - \ddot{\mathcal{X}}^r + \mathcal{D}_x(t)] \\ &- c_5 e_y^2(t) + e_y(t)e_{yy}(t) + \mathcal{S}_x(t)[(k_y + c_5)\dot{e}_x(t) \\ &+ v_y - \ddot{\mathcal{Y}}^r + \mathcal{D}_x(t)] \end{aligned}$$

From (16), (22), (23), (24), **we can obtain,**

$$\dot{V}_T \leq -\mathcal{E}_1^T Q_\phi \mathcal{E}_1 - \mathcal{E}_2^T Q_\theta \mathcal{E}_2 - \mathcal{E}_3^T Q_\psi \mathcal{E}_3 \quad \leq 0 \tag{26}$$

where $e_{xx}(t) = \dot{\mathcal{X}}_1 - \mathcal{X}_2^r$, $e_{yy}(t) = \dot{\mathcal{Y}}_1 - \mathcal{Y}_2^r$, $\mathcal{X}_2^r(t) = \dot{x}^r(t) - c_3 e_x(t)$ and $\mathcal{Y}_2^r(t) = \dot{y}^r(t) - c_5 e_y(t)$. According to the aforesaid analysis, the outer-loop stability is ensured. □

3.2. Attitude Controller

In this section, a FO fast terminal sliding mode controller will be designed for attitude subsystem. First, let us consider the roll subsystem as :

$$\begin{aligned}
\dot{\Phi}_1(t) &= \Phi_2(t) \\
\dot{\Phi}_2(t) &= \frac{\mathbf{I}_2 - \mathbf{I}_3}{\mathbf{I}_1}\dot{\theta}(t)\dot{\psi}(t) - \frac{\varpi J_r}{\mathbf{I}_1}\dot{\theta}(t) - \frac{K_1}{\mathbf{I}_1}\dot{\phi}^2(t) \\
&\quad + \frac{1}{\mathbf{I}_1}\mathcal{M}_{xx} + \mathcal{D}_\phi(t)
\end{aligned} \tag{27}$$

where $\Phi_1(t)$ and $\Phi_2(t)$ represent the state variable of roll subsystem. Let the roll error be as:

$$e_\phi(t) = \Phi_1(t) - \phi^r(t) \tag{28}$$

A FOTSM manifold is presented as,

$$\begin{aligned}
\mathcal{S}_\phi(t) &= \beta_\phi I^{\alpha_\phi} e_\phi(t) + \gamma_\phi D^{1-\alpha_\phi}[K_{\phi 1} e_\phi(t) \\
&\quad + K_{\phi 2} sig(e_\phi^{\mu_\phi}(t))] + D^{1-\alpha_\phi}\dot{e}_\phi(t)
\end{aligned} \tag{29}$$

where $\alpha_\phi \in]0,1[$, β_ϕ and γ_ϕ, $K_{\phi 1}$, and $K_{\phi 2}$ are positive coefficients.

Tacking fractional derivative of the sliding variable yields:

$$\begin{aligned}
D^{\alpha_\phi}\mathcal{S}_\phi(t) &= \beta_\phi e_\phi(t) + \gamma_\phi D^1[K_{\phi 1} e_\phi(t) \\
&\quad + K_{\phi 2} sig(e_\phi^{\mu_\phi}(t))] + \ddot{e}_\phi(t)
\end{aligned} \tag{30}$$

Hence, one has

$$\begin{aligned}
D^{\alpha_\phi}\mathcal{S}_\phi(t) &= \beta_\phi e_\phi(t) + \gamma_\phi D^1[K_{\phi 1} e_\phi(t) \quad + K_{\phi 2} sig(e_\phi^{\mu_\phi}(t))] \\
&\quad + \frac{\mathbf{I}_2 - \mathbf{I}_3}{\mathbf{I}_1}\dot{\theta}(t)\dot{\psi}(t) - \frac{\varpi J_r}{\mathbf{I}_1}\dot{\theta}(t) - \frac{K_1}{\mathbf{I}_1}\dot{\phi}^2(t) \\
&\quad + \frac{1}{\mathbf{I}_1}\mathcal{M}_{xx} + \mathcal{D}_\phi(t)
\end{aligned} \tag{31}$$

From (30), one gets the following equivalent control law

$$\begin{aligned}\mathcal{M}_{xxe} = -\mathbf{I}_1[\beta_\phi e_\phi(t) + \gamma_\phi D^1[K_{\phi 1} e_\phi(t) \quad + K_{\phi 2} sig(e_\phi^{\mu_\phi}(t))] \\ + \frac{\mathbf{I}_2 - \mathbf{I}_3}{\mathbf{I}_1}\dot{\theta}(t)\dot{\psi}(t) - \frac{\varpi J_r}{\mathbf{I}_1}\dot{\theta}(t) - \frac{K_1}{\mathbf{I}_1}\dot{\phi}^2(t)]\end{aligned} \tag{32}$$

Assumption 2. ***The disturbance on the roll dynamics is satisfied*** $\|\mathcal{D}_\phi\| \leq I^{1-\alpha_\phi}\delta_{\mathcal{D}_\phi}$ ***or*** $\left\|D^{1-\alpha_\phi}\mathcal{D}_\phi\right\| \leq \delta_{\mathcal{D}_\phi}$ ***where*** $\delta_{\mathcal{D}_\phi}$ ***is a positive function. There is an upper constraint on the time derivative of disturbances because during quadrotor flight, the environment disturbances, such as turbulence and gusts, are energy constrained and cannot last for a long period. A FO derivative of disturbances is taken into consideration in this paper.***

The following Lemma is introduced in order to get the approximated form of the fractional calculus answer.

Lemma 2. ***In Ref. [26], suppose that*** $\hbar_1$, $\hbar_2 > 1$, ***and*** $\frac{1}{\hbar_1} + \frac{1}{\hbar_2} = 1$, ***if*** $|\kappa_1(*)|^{\hbar_1}$, $|\kappa_2(*)|^{\hbar_2} \in L^1(D)$, ***then*** $\kappa_1(*)\kappa_2(*) \in \mathbb{L}^1(D)$ ***and***

$$\int_D |\kappa_1(x)\kappa_2(x)|dx \leq \left(\int_D |\kappa_1(x)|^{\hbar_1}dx\right)^{\frac{1}{\hbar_1}} \left(\int_D |\kappa_2(x)|^{\hbar_2}dx\right)^{\frac{1}{\hbar_2}} \tag{33}$$

where $L^1(D)$ ***stands for the Banach space of all Lebesgue measurable functions*** $\kappa_1 : D \to \mathbb{R}$ ***with*** $\int_D |\kappa_1(x)|dx < \infty$.

Since fractional calculus has a memory, it is necessary to know the previous values of all the variables throughout an infinite time span in order to calculate the fractional derivative of the variable $x(t)$**. Consequently, the ensuing presumption is presented.**

Remark 3. ***Assumption 2 states that the perturbation is bounded by a known function to be designed using Lemma 2. It is based on the fact that most input physical systems are limited by motor converters. Hence, the control input can change over time but cannot be infinite. As mentioned in [24], although being conservative, it may nonetheless cover a wide range of practical applications. We should***

also mention that Assumption 2 is based on the fact that the generalized version of the second-order nonlinear dynamical system has been studied like as the subsystem of the quadrotor. It should be noted that this Assumption 2 is strict as it can still be applied to a variety of dynamical systems in the literature, including robotic systems [24] and quadrotor systems [27, 28].

Remark 4. ***Assumption 2 studies the bounded disturbances using a positive function to present the upper bounded of the disturbance and uncertainty on the QUAV dynamics. Similar assumptions can be found in [24, 27, 28].***

To improve the tracking performance against disturbances, we define the switching law as follows:

$$\mathcal{M}_{xxs} = -\mathbf{I}_1[I^{1-\alpha_\phi}\delta_{\mathcal{D}_\phi} + \varepsilon_\phi sig^{q_\phi}(\mathcal{S}_\phi(t)) + \sigma_\phi I^{1-\alpha_\phi}\mathcal{S}_\phi(t)] \tag{34}$$

where $q_\phi \in]0,1[$, ε_ϕ and σ_ϕ are positive parameters. Thus, the proposed control law for the roll subsystem under model uncertainties/disturbances is

$$\mathcal{M}_{xx} = \mathcal{M}_{xxe} + \mathcal{M}_{xxs} \tag{35}$$

Theorem 3. *The origin of* ***roll attitude system presented in Table 1****, with Assumption 2, under the designed controller in* (35) *and using the the sliding variable* $\mathcal{S}_\phi(t)$*, is finite-time stable with* $\mathbf{t}_r <= \frac{1}{\sigma_\phi(1-q_\phi)} ln(1 + \frac{\sigma_\phi}{\varepsilon_\phi}\|\mathcal{S}_\phi(0)\|_2^{1-q_\phi})$.

Proof. Define the LF candidate for the $\phi(t)$-subsytem as

$$V_\phi(t) = \frac{1}{2}\mathcal{S}_\phi^2(t) \tag{36}$$

The time-derivative of $V_\phi(t)$ is,

$$\dot{V}_\phi(t) = \mathcal{S}_\phi(t)\dot{\mathcal{S}}_\phi(t) = \mathcal{S}_\phi(t)D^{1-\alpha_\phi}(D^{\alpha_\phi}\mathcal{S}_\phi(t)) \tag{37}$$

Substituting (31) **and** (35) into (37), one gets

$$\begin{aligned}\dot{V}_\phi(t) &= \mathcal{S}_\phi(t)D^{1-\alpha_\phi}(\mathcal{D}_\phi(t) - I^{1-\alpha_\phi}\delta_{\mathcal{D}_\phi} - I^{1-\alpha_\phi}\varepsilon_\phi sig^{q_\phi}\mathcal{S}_\phi(t) \\ &\quad - \sigma_\phi I^{1-\alpha_\phi}\mathcal{S}_\phi(t)) \\ &= \mathcal{S}_\phi(t)(D^{1-\alpha_\phi}\mathcal{D}_\phi(t) - \delta_{\mathcal{D}_\phi} - \varepsilon_\phi sig^{q_\phi}\mathcal{S}_\phi(t) - \sigma_\phi\mathcal{S}_\phi(t))\end{aligned} \tag{38}$$

Using Assumption 2, one get

$$\dot{V}_\phi(t) \leq -\varepsilon_\phi|\mathcal{S}_\phi(t)|^{1+q_\phi} - \sigma_\phi\mathcal{S}_\phi^2(t) \tag{39}$$

Hence, one obtains

$$\dot{V}_\phi(t) \leq -\varepsilon_\phi|\mathcal{S}_\phi|^{1+q_\phi}(t) \tag{40}$$

The above inequality (40) can be rewritten as

$$\dot{V}_\phi(t) \leq -\varepsilon_\phi\|\mathcal{S}_\phi(t)\|_2^{1+q_\phi} \tag{41}$$

Using Eq. (39), one has

$$\begin{aligned}\dot{V}_\phi(t) &= -\varepsilon_\phi|\mathcal{S}_\phi(t)|^{1+q_\phi} - \sigma_\phi\mathcal{S}_\phi(t)^2 \\ &= -\varepsilon_\phi(2V_\phi(t))^{\frac{1+q_\phi}{2}} - \sigma_\phi(2V_\phi(t))\end{aligned} \tag{42}$$

As a result, a simple calculation yields,

$$\begin{aligned}dt &= -\frac{dV_\phi(t)}{\varepsilon_\phi(2V_\phi(t))^{\frac{1+q_\phi}{2}} + \sigma_\phi(2V_\phi(t))} \\ &= -\frac{1}{2}\frac{(2V_\phi(t))^{-\frac{1}{2}}d(2V_\phi(t))}{\varepsilon_\phi(2V_\phi(t))^{\frac{q_\phi}{2}} + \sigma_\phi(2V_\phi(t))^{\frac{1}{2}}} \\ &= -\frac{d(2V_\phi(t))^{\frac{1}{2}}}{\varepsilon_\phi(2V_\phi(t))^{\frac{q_\phi}{2}} + \sigma_\phi(2V_\phi(t))^{\frac{1}{2}}} \\ &= \frac{d\|\mathcal{S}_\phi(t)\|_2}{\varepsilon_\phi\|\mathcal{S}_\phi(t)\|_2^{q_\phi} + \sigma_\phi\|\mathcal{S}_\phi(t)\|_2} \\ &= \frac{\|\mathcal{S}_\phi(t)\|_2^{-q_\phi}d\|\mathcal{S}_\phi(t)\|_2}{\varepsilon_\phi + \sigma_\phi\|\mathcal{S}_\phi(t)\|_2^{1-q_\phi}} \\ &= \frac{1}{\sigma_\phi(1-q_\phi)}\frac{d(\sigma_\phi\|\mathcal{S}_\phi(t)\|_2^{1-q_\phi}}{\varepsilon_\phi + \sigma_\phi\|\mathcal{S}_\phi(t)\|_2^{1-q_\phi}}\end{aligned} \tag{43}$$

Taking integral of both sides of Eq. (43) from 0 to $\mathbf{t}_r$ and $\mathcal{S}_\phi(\mathbf{t}_r) = 0$, one gets

$$\int_0^{\mathbf{t}_r} dt = \frac{1}{\sigma_\phi(1-q_\phi)} \int_0^{\mathbf{t}_r} \frac{d(\sigma_\phi \|\mathcal{S}_\phi(t)\|_2^{1-q_\phi}}{\varepsilon_\phi + \sigma_\phi \|\mathcal{S}_\phi(t)\|_2^{1-q_\phi}}$$
$$t_r = \frac{1}{\sigma_\phi(1-q_\phi)} ln(1 + \frac{\sigma_\phi}{\varepsilon_\phi} \|\mathcal{S}_\phi(0)\|_2^{1-q_\phi}) \tag{44}$$

This completes the proof. □

Similarly to the roll controller, the pitch and yaw control laws can be given as:

$$\begin{aligned}\mathcal{M}_{yy} = &-\mathbf{I}_2[\beta_\theta e_\theta(t) + \gamma_\theta D^1[K_{\theta 1} e_\theta(t) \quad + K_{\theta 2} sig(e_\theta^{\mu_\theta}(t))] \\ &+ \frac{\mathbf{I}_3 - \mathbf{I}_1}{\mathbf{I}_2} \dot{\phi}(t)\dot{\psi}(t) + \frac{\varpi J_r}{\mathbf{I}_2} \dot{\phi}(t) - \frac{K_2}{\mathbf{I}_2} \dot{\theta}^2(t)] \\ &- \mathbf{I}_2[I^{1-\alpha_\theta} \delta_{\mathcal{D}_\theta} + \varepsilon_\theta sig^{q_\theta}(\mathcal{S}_\theta(t)) + \sigma_\theta I^{1-\alpha_\theta} \mathcal{S}_\theta(t)]\end{aligned} \tag{45}$$

and

$$\begin{aligned}\mathcal{M}_{zz} = &-\mathbf{I}_3[\beta_\psi e_\psi(t) + \gamma_\psi D^1[K_{\psi 1} e_\psi(t) \quad + K_{\psi 2} sig(e_\psi^{\mu_\psi}(t))] \\ &+ \frac{\mathbf{I}_1 - \mathbf{I}_2}{\mathbf{I}_3} \dot{\phi}(t)\dot{\theta}(t) - \frac{K_3}{\mathbf{I}_3} \dot{\psi}^2(t)] \\ &- \mathbf{I}_3[I^{1-\alpha_\psi} \delta_{\mathcal{D}_\psi} + \varepsilon_\psi sig^{q_\psi}(\mathcal{S}_\psi(t)) + \sigma_\theta I^{1-\alpha_\psi} \mathcal{S}_\psi(t)]\end{aligned} \tag{46}$$

where $\alpha_\theta, \alpha_\psi \in]0,1[^2$. β_ϕ, γ_ϕ, $K_{\phi 1}$, $K_{\phi 2} > 0$. $q_\theta, q_\psi \in]0,1[^2$, $\varepsilon_\theta, \varepsilon_\psi$ and σ_θ, σ_ψ are positive parameters. Figure 3 represents the flowchart diagram of the FOFTSMC proposed in this paper.

Theorem 4. *The origin of the attitude system* ***presented in Table 1****, with Assumption 2,* ***the designed controllers in*** (35)**,** (45)**,** (46) *and the nonlinear sliding variables* $\mathcal{S}_\phi(t), \mathcal{S}_\theta(t)$*, and* $\mathcal{S}_\psi(t)$*, is finite-time stable.*

Proof. Consider the candidate Lyapunov function for the attitude as follows:

$$V_R = \frac{1}{2}\mathcal{S}_\phi^2(t) + \frac{1}{2}\mathcal{S}_\theta^2(t) + \frac{1}{2}\mathcal{S}_\psi^2(t) \tag{47}$$

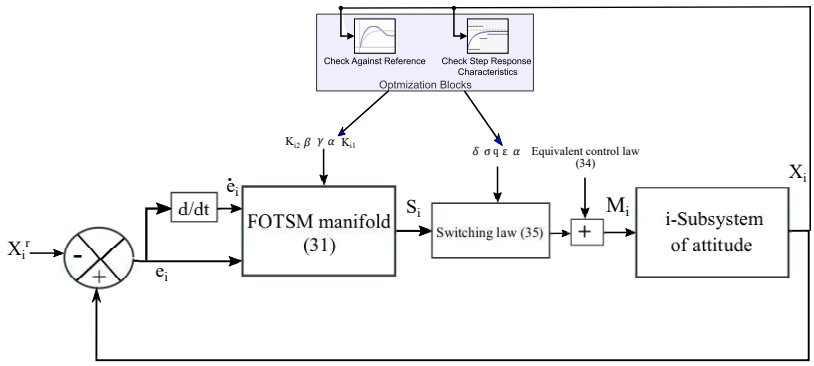

Figure 3: The flowchart diagram of the proposed FOFTSMC controller.

The time-derivative of V_R is given by:

$$\begin{aligned}\dot{V}_R =& \mathcal{S}_\phi(t)\dot{\mathcal{S}}_\phi(t) + \mathcal{S}_\theta(t)\dot{\mathcal{S}}_\theta(t) + \mathcal{S}_\psi(t)\dot{\mathcal{S}}_\psi(t) \\ =& \mathcal{S}_\phi(t)D^{1-\alpha_\phi}(D^{\alpha_\phi}\mathcal{S}_\phi(t)) + \mathcal{S}_\theta(t)D^{1-\alpha_\theta}(D^{\alpha_\theta}\mathcal{S}_\theta(t)) + \mathcal{S}_\psi(t)D^{1-\alpha_\psi}(D^{\alpha_\psi}\mathcal{S}_\psi(t))\end{aligned}$$

According to Assumption 2 and from (31), (35), (39), (45), (46), we can obtain,

$$\begin{aligned}\dot{V}_R \leq& -\varepsilon_\phi|\mathcal{S}_\phi(t)|^{1+q_\phi} - \sigma_\phi\mathcal{S}_\phi^2(t) - \varepsilon_\theta|\mathcal{S}_\theta(t)|^{1+q_\theta} - \sigma_\theta\mathcal{S}_\theta^2(t) - \varepsilon_\psi|\mathcal{S}_\phi(t)|^{1+q_\psi} - \sigma_\psi\mathcal{S}_\psi^2(t) \\ \leq& 0\end{aligned} \tag{48}$$

The reaching condition of attitude loop stability is ensured. Then, using the results of Theorem 3, of the origin of the attitude loop is finite-time stable. □

Corollary 1. *Considered overall system* ***presented in Table 1 in the presence of disturbances using the ultimate control laws, presented in*** (16), (23), (24), (35), (45), ***and*** (46), *the sliding mode variables be reached in the finite-time, then the tracking errors for both attitude and position converge to zero in a finite-time.*

Proof. The Lyapunov function for the quadrotor system is chosen as follows:

$$V_S = V_R + V_T \tag{49}$$

The time-derivative of V_S is given by:

$$\dot{V}_S = \dot{V}_R + \dot{V}_T \tag{50}$$

Based on the results of proof of the theorem 2 and 4 in order to proof Corollary 1. Then from (26) **and** (48)**, we have,** □

$$\begin{aligned}\dot{V}_S \leq & -\varepsilon_\phi|\mathcal{S}_\phi(t)|^{1+q_\phi} - \sigma_\phi\mathcal{S}_\phi^2(t) - \varepsilon_\theta|\mathcal{S}_\theta(t)|^{1+q_\theta} - \sigma_\theta\mathcal{S}_\theta^2(t) - \varepsilon_\psi|\mathcal{S}_\phi(t)|^{1+q_\psi} - \sigma_\psi\mathcal{S}_\psi^2(t) \\ & - \mathcal{E}_1^T Q_\phi \mathcal{E}_1 - \mathcal{E}_2^T Q_\theta \mathcal{E}_2 - \mathcal{E}_3^T Q_\psi \mathcal{E}_3 \\ & \leq 0\end{aligned} \tag{51}$$

The Lyapunov technique is used to **demonstrate the global stability of rotational and translational tracking errors.**

Remark 5. *The proposed control method is based on backstepping with FTSMC, wich show finite-time convergence of the QUAS state variables and robustness against parametric uncertainties and disturbances; FO control have the capability to choose the fractional operators; FOFTSMC provides the finite-time stability and compensates the effects of disturbances.*

Remark 6. *The proposed attitude control is an improved version of FOSMC presented by the authors of [24].* ***In addition, the proposed control laws presented in*** (35)***,*** (45)***, and*** (46) ***have a flexible choice of FO parameters of the derivatives and integrators (*** α ***and*** q***).***

The control law signals v_x, v_y, v_z, $\mathcal{M}_{xx}$, $\mathcal{M}_{yy}$, and $\mathcal{M}_{zz}$ are modified by the saturation function below

$$\mathcal{M}_i = sat(\mathcal{M}_{iL}, \bar{\mathcal{M}}_i, \tau_{iL}) = \begin{cases} \mathcal{M}_{iL} & \bar{\mathcal{M}}_i \quad < \mathcal{M}_{iL} \\ \bar{\mathcal{M}}_i & \mathcal{M}_{iL} < \mathcal{M}_{iL} < \mathcal{M}_{iU} \\ \mathcal{M}_{iU} & \bar{\mathcal{M}}_i \quad > \mathcal{M}_{iU} \end{cases} \tag{52}$$

where $\mathcal{M}_{iL}$ and $\mathcal{M}_{iU}$ are the four control inputs' lower and upper limit bounds, respectively. **In this paper, the saturation function** (52) **applied for the four inputs is used to reduce oscillation and amplitudes of the inputs of the system Ref. [29].**

Remark 7. ***In this paper two nonlinear surfaces are proposed in order to obtain the finite-time convergence of the quadrotor states.***

Remark 8. *The advantages of the proposed fractional-order finite-time sliding mode controllers: finite-time convergence of the system states, finite-time convergence in the reaching phase, reduction of chattering phenomenon, offers an extra FO differential element into the existing one insensitive to bounded external disturbances and parametric uncertainties.*

Remark 9. *The proposed control method's implementation challenges for quadrotor position and attitude will be examined from four simulations. First, the complexity of the problem is due to the fact that for position and attitude, tracking performance such as convergence time and steady-state performance are considered, while the time-varying disturbances, parameter uncertainties (such as air drag coefficients), and external disturbances exist. Second, the novelty and difficulty of the proposed method can be broken down to the following two points.*

- *For position control, an flexible FO backstepping TSMC is constructed and employed different from [22], which enhanced the tracking performance against random external disturbances and random drag coefficients.*
- *For attitude control, a finite-time controller based on fractional-order fast terminal sliding mode control is developed, which enhanced the robustness and accuracy the rotational subsystem.*

The disadvantages of the proposed scheme can be defined as: requires complex adaption laws, complexity in coefficient calculation, and selection of nonlinear surfaces is cumbersome in order to avoid the singularity problem.

4. Simulation results and discussions

In this part, the protocol of simulations will be discussed. Simulator implements dynamics presented **in Table 1**. This dynamic included the forces and momentums. The variation of the drag coefficients and external disturbances are taken account to make simulate realistic quadrotor in order validate the proposed FO controllers. The mathematical models of the sensors, actuators, and the plant refer to [3, 30] and the selected physic parameters of the QUAS are [28], $\mathbf{m} = 2kg$, $\mathbf{I} = diag[16, 16, 32]10^{-3}kg.m^2$, $K_{\mathcal{P}} = diag[0.1, 0.1, 0.1]10^{-1}Nsm^{-1}$, $K_{\Psi} = diag[12, 12, 12]10^{-3}Nsrad^{-1}$, $g = 9.8m/s^2$, $\hbar_b = 2.984210^{-3}Ns^2$, and $\hbar_c = 3.232010^{-2}Nms^2$. The initial conditions $[0.5, 0.1, 0]10^{-1}m$ and $[1, 1, 1]10^{-2}rad$ have been considered in all scenarios. To obtain signification tracking performance, the FOHFTC parameters are tuned. In order to highlight the present results, a comparison study is presented using two controllers. In the following subsections, we present the results these scenarios with discussion.

Control parameters selection

In this part, the parameters selection of the suggested control method will be discussed in order to implement this controller.

(A) For outer loop (position controller)

- Selection of c_j for $j = 1, 2, 3$: this parameter increases the stability of tracking errors. The latter depends on the initial conditions of the state of the system.
- Selection of k_j, μ_j: these parameters affect directly the sliding mode dynamics as presented in (13). A faster convergence to zero of the tracking errors can be obtained by choosing a big value of those parameters but increase the input signals.
- Selection of c_i: it is fractional operator which used to improve the robustness.
- Selection of h_{j1}, h_{j2}: these parameters are positive gains designed in the reaching law (15) to achieve a high level of robustness.

Table 2: Control system parameters.

Position parameters loop	Values
c_j, h_1, h_2	4, 1, 6
μ_j, q_j, k	0.9, 0.7, 10
Attitude parameters loop	**Values**
σ, α, β,	0.6, 0.98, 0.1224
q_i, ε, γ_i	0.7, 35.6089, 39.3958
μ_i, K_{i1}, K_{i2}	0.9, 5, 12

(B) For inner loop (attitude controller)

- Selection of $\beta_i, \alpha_i, \gamma_i, k_i, \mu_i$ for $i = \phi, \theta, \psi$ for $i = \phi, \theta, \psi$: these parameters affect directly the sliding mode dynamics as presented in (29). A faster convergence to zero of the tracking errors can be obtained by choosing a big value of those parameters but increase the input signals.
- Selection of $\sigma_i, \varepsilon_i, q_i$: these coefficients are designed in the reaching control law (34) to obtain a high level of robustness against parameters uncertainties and disturbances.

(C) Selection of parameters in the simulations. The following remark gives the method used to obtain the parameter controllers.

Remark 10. *The controller settings are fine-tuned to meet the quadrotors performance requirements. Furthermore, the Simulink software's optimization toolbox is utilized to determine the optimum values for these parameters. (see Ref. ([31]).*

The control parameters are given in Table 2.

According to Lemma 2, we can write the fractional estimation of "disturbance term" as $\delta_{Di} = (\frac{\pi}{\Gamma(\alpha_i)})(\Gamma(\alpha_i)(1-\alpha_i^2)\Gamma(\alpha_i^2))^{\frac{1}{1+\alpha_i}}(\frac{t^{1+\alpha_i}}{1+\alpha_i})^{\frac{\alpha_i}{1+\alpha_i}}$**.**

Approximation of the FO derivatives

The FO approximation that was used in the simulation will be introduced in this part of the paper. Complications in practical implementation of fractional-order derivative and integrator terms are one of the challenges that have been encountered in applications and simulations of these types of operators. This explains why only integer-order derivatives and integrals are used to approximate fractional-order derivative and integrator terms [32, 33]. In the literature, the Crone approximation is the most used method to simulate the FO operators developed in the proposed controllers (see Refs. [34, 35] and the references therein). A recursive distribution of poles and zeros within a frequency range $[\omega_l, \omega_h]$ is used in this approximation. The higher the order N, the more exact the approximation of fractional dynamics in the frequency range $[\omega_l, \omega_h]$ becomes. Original mathematical concepts based on this approximation were included in the CRONE toolbox, which has been developed by the CRONE team since the 1990s and is a MATLAB toolbox dedicated to the fractional calculus and its applications in automatic control and signal processing.

Remark 11. *In this paper, the Oustaloup modified filter is used to approximate the FO terms. The frequency range is 0.01 to 100 rad/s with 10 orders.*

To show clearly the superiority of the suggested hybrid control method and to verify its advantages, four scenarios in terms of disturbances are considered under different paths following.

4.1. Simulations with slowly time-varying disturbances

In this subsection, we conduct a simulation in the case of random uncertainties on the drag coefficients, including both translational and rotational subsystems. The effect is shown in Fig. 4, which approximates to a real flight.

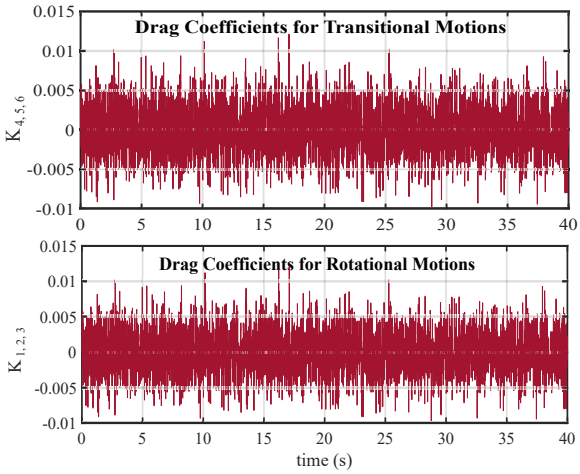

Figure 4: The imitated drag coefficients.

The chosen disturbances in this case are

$$\mathcal{D}_x(t) = \begin{cases} 0 \quad m/s^2 \quad t \in [0, 10] \\ \frac{1}{2} \quad m/s^2 \quad t \in [0, 155] \end{cases}$$

$$\mathcal{D}_y(t) = \begin{cases} 0.4 \quad m/s^2 \quad t \in [0, 20] \\ -0.2 \quad m/s^2 \quad t \in [20, 50] \\ 0.2 \quad m/s^2 \quad t \in [50, 155] \end{cases}$$

$$\mathcal{D}_z(t) = \begin{cases} 0 \quad m/s^2 \quad t \in [0, 10] \\ -2 \quad 10^{-1} m/s^2 \quad t \in [10, 40] \\ 3 \quad 10^{-1} m/s^2 \quad t \in [40, 155] \end{cases}$$

$$\mathcal{D}_\phi(t) = \frac{1}{2}\cos\left(\frac{1}{2}t\right) + \tanh(0.3t) \quad rad.s^{-2}$$

$$\mathcal{D}_\theta(t) = \frac{1}{2}\cos(t) + \cos(0.3t) \quad rad.s^{-2}$$

$$\mathcal{D}_\psi(t) = \frac{1}{2}\sin(0.7t) + 2 \quad rad.s^{-2} \tag{53}$$

Figure 5 shows the results of position tracking, and Figure 6 depicts the attitude tracking. Based on these results, the QUAS tracks the desired path with accuracy under disturbances and the change of drag coefficients after a short period.

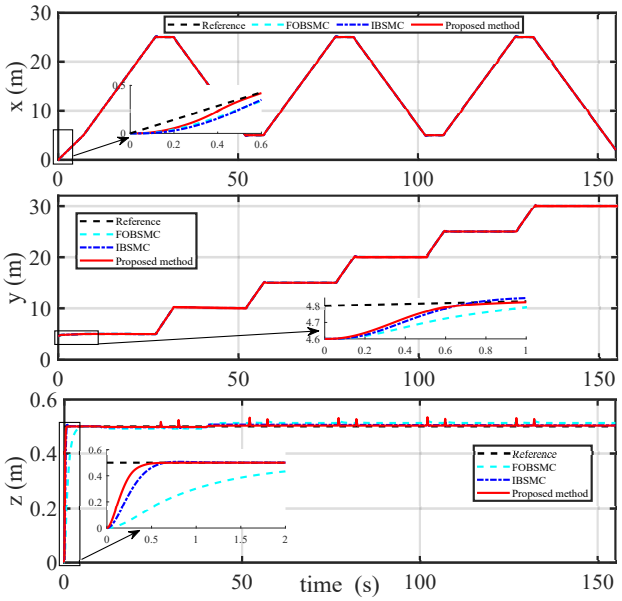

Figure 5: Position tracking performance comparison with [22] and [36] control methods.

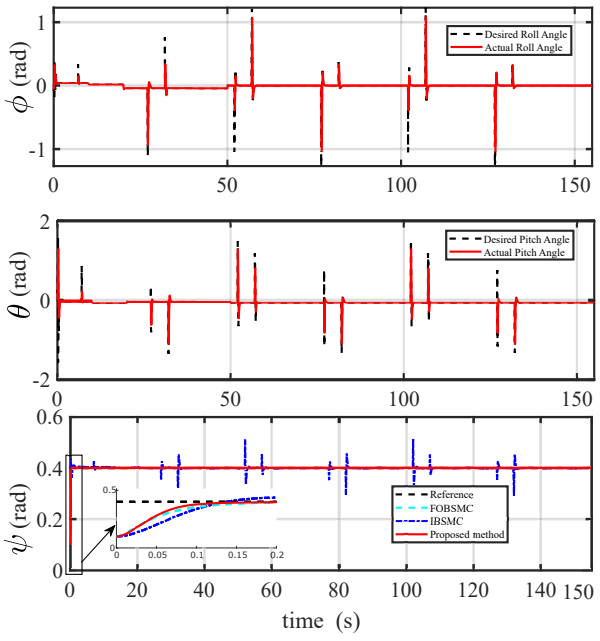

Figure 6: Attitude tracking performance comparison with [22] and [36] control methods.

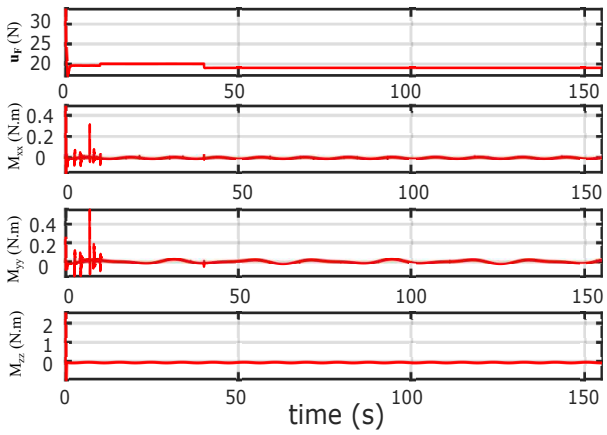

Figure 7: Control inputs.

Figure 8 depicts the time-history of the tracking errors. The simulation demonstrates the uniform tracking performances in terms of steady states, rejection of disturbances, fast responses and speed. Figure 7 shows the responses of the control inputs are chattering-free, and its amplitudes have appropriate values. The path following in 2D and 3D spaces is depicted respectively in the Figures 10 and 9. As can be seen, the suggested controller is capable of controlling the QUAS in the presence of perturbation/uncertainty.

The disturbances and uncertainties applied on both rotational and translational subsystems decrease tracking performance in path following of the QUAS using classical control methods. As result, the FO control method proposed here has better tracking performances and the ability to cope with these perturbations compared with [22] and [36] as shown in Fig. 5.

4.2. Simulations with random Gaussian disturbances

In this subsection, another scenario is proposed tacking account the random Gaussian disturbances for both attitude/position as shown in Fig. 11.

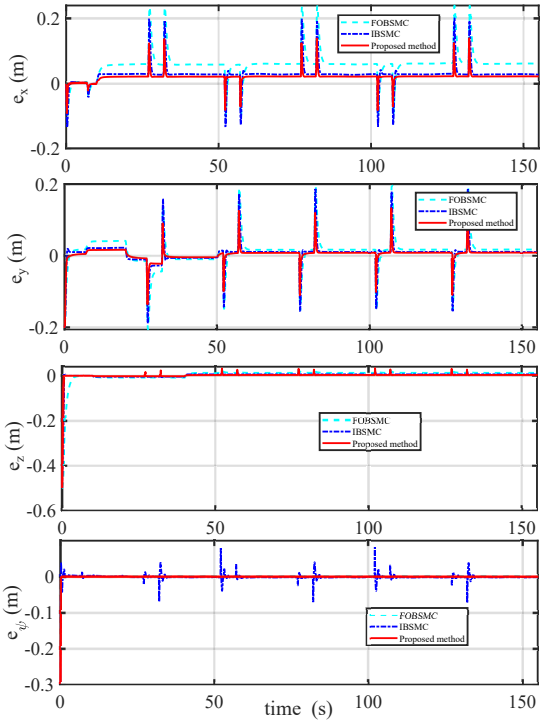

Figure 8: Tracking performance errors comparison with [22] and [36] control methods.

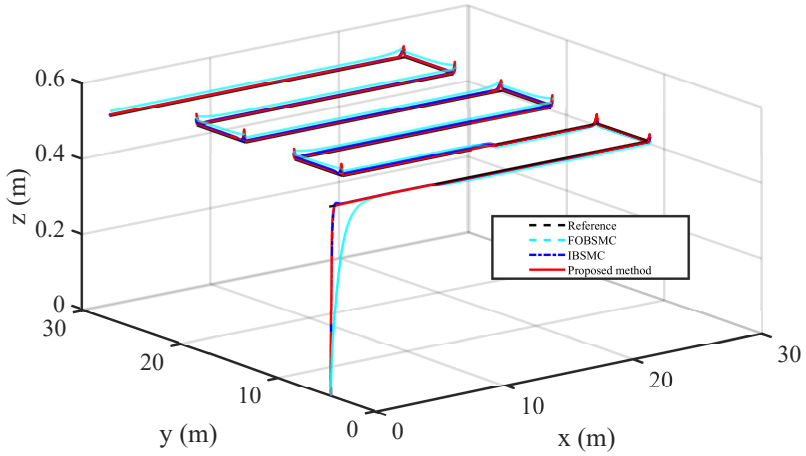

Figure 9: 3D trajectory tracking performance comparison with [22] and [36] control methods.

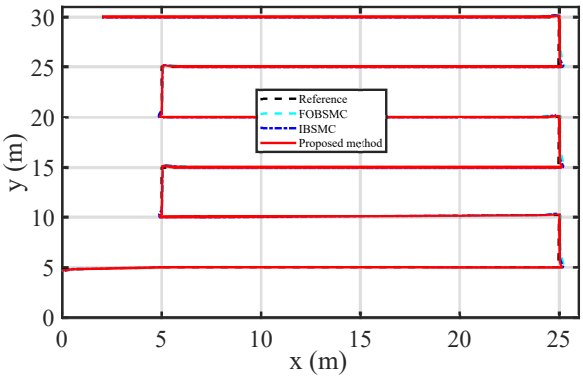

Figure 10: 2D trajectory tracking performance comparison with [22] and [36] control methods.

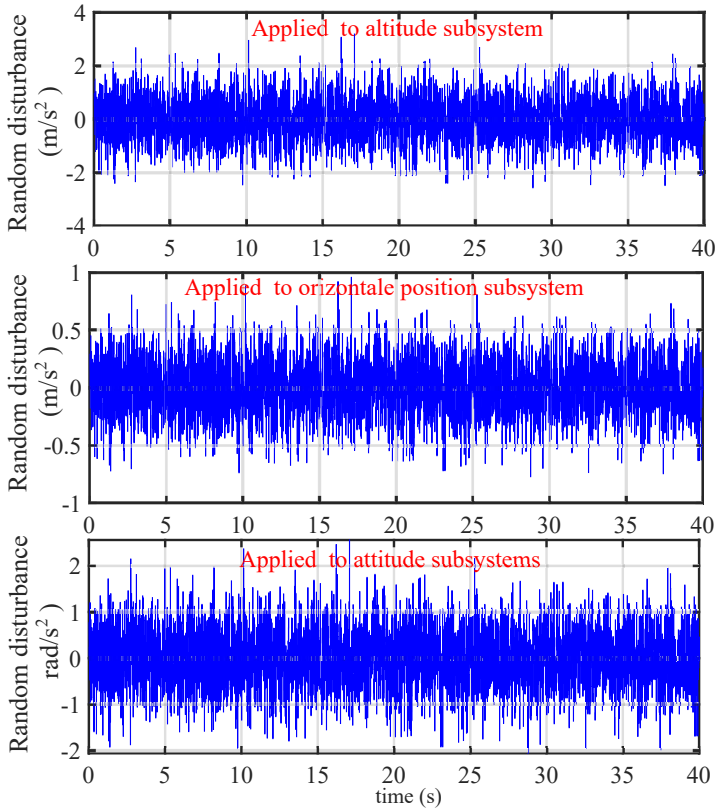

Figure 11: Gaussian random disturbances.

The reference trajectory is chosen as :

$$x^r(t) = \frac{1}{2}\cos\Big(\frac{\pi}{20}\Big)m, \quad y^r(t) = \frac{1}{2}\sin\Big(\frac{\pi}{20}\Big)m \tag{54}$$

$$z^r(t) = 2 - 2\cos\Big(\frac{\pi}{2}\Big)m, \quad \psi^r = \frac{1}{2}rad \tag{55}$$

The results in this case using the FOHFTC proposed in this work, control methods proposed in [22], and [36] are plotted in Figs. 12 to 16.

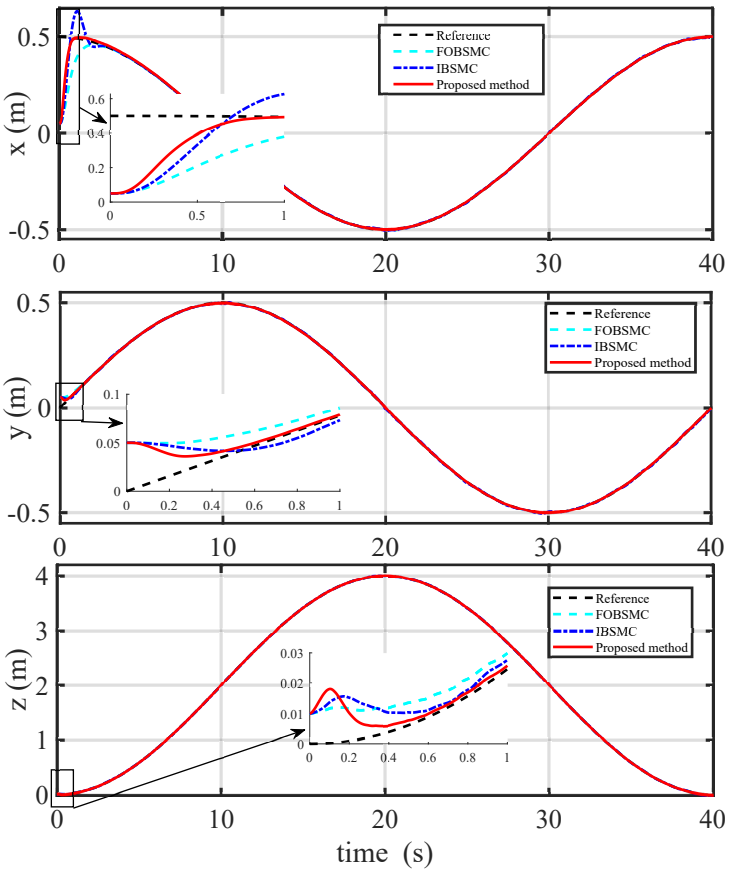

Figure 12: Position tracking performance comparison with [22] and [36] control methods.

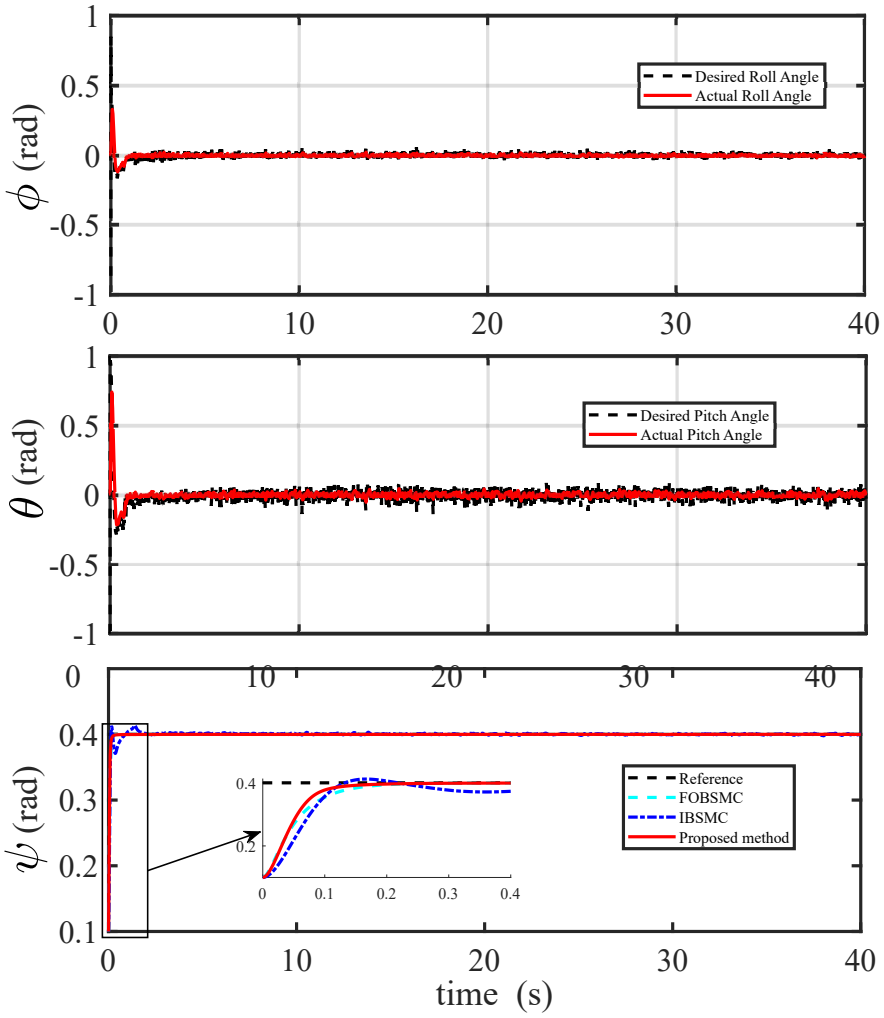

Figure 13: Attitude tracking performance comparison with [22] and [36] control methods.

The position, as can be observed, converges to the intended trajectory in a finite amount of time. The attitude tracking is shown in Fig. 13. As can be observed, the roll/pitch angle converges to the origin, and the yaw angle tracks the desired value with accuracy. Note that, the control performance in the inner-loop (attitude loop) enhanced the position tracking. The tracking errors in the position loop and tracking error of the yaw angle are shown in Fig. 15. As can be seen, these errors converge to the origin with a short finite time and

maintain steadily in the neighborhood of origin.

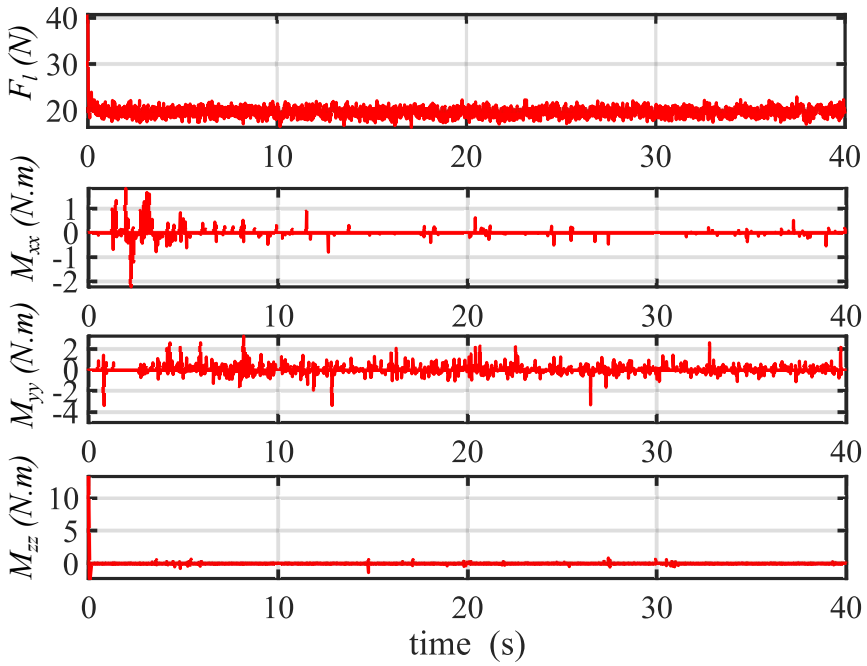

Figure 14: Control inputs.

Figure 14 depicts the applied control inputs. As can be observed from these results, the inputs are smooth and converge to their values.

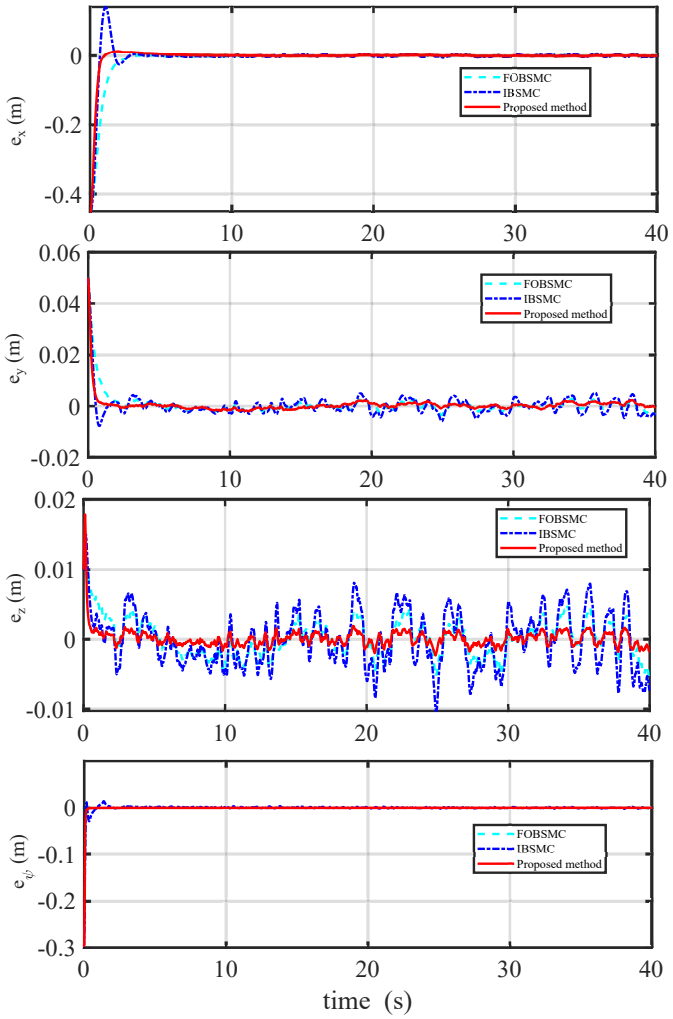

Figure 15: Tracking errors performance comparison with [22] and [36] control methods.

The 2D trajectory-tracking performance is depicted in Fig. 16 and 3D path-following is shown in Fig. 17. As can be seen, the trajectories in 2D and 3D spaces track the desired trajectories with high precision. In addition, the effect of the random Gaussian disturbances applied on the translational and rotational loops can be precisely compensated using the designed FOHFTC.

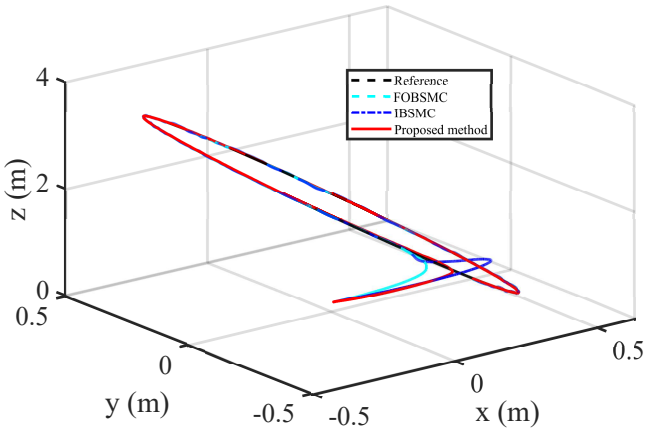

Figure 16: 3D trajectory tracking performance comparison with [22] and [36] control methods.

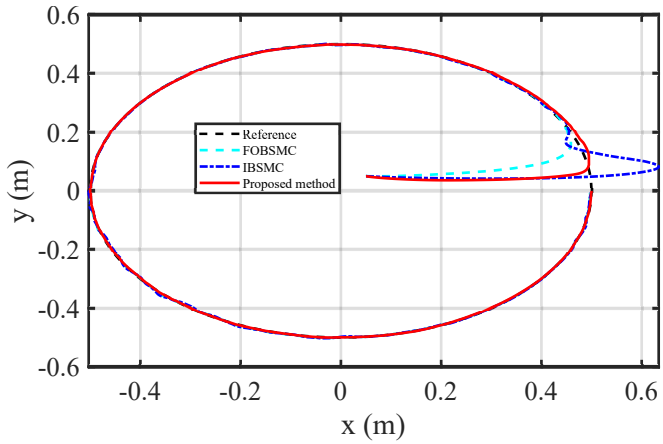

Figure 17: 2D trajectory tracking performance comparison with [22] and [36] control methods.

More importantly, the proposed control method achieves a better tracking of the desired trajectory without chattering phenomenon and enhances the tracking performance against random Gaussian disturbances.

4.3. Comparison with fractional-order backstepping sliding mode control scheme proposed in [22]

In summary, the tracking performance obtained in scenario 1, Figs. 5, 6, and 8 show good of the control scheme proposed in this work. Nonetheless, for the

control objective of rejecting the disturbances during the flight and following the desired trajectory, the proposed nonlinear control law was found to perform better than the FO control law developed in [22]. Figures 9 and 10 demonstrate this performance in term of tracking performance.

The convergence obtained by the proposed control method is better than the results obtained from the control scheme suggested in [22]. For example, the settling time produced by the proposed control method is small than other FOBSMC as presented in Figs. 5 and 9. It can be seen from Fig. refAttitude1, the orientation dynamics are quickly regulated using the proposed control approach.

Concerning the scenario 2, the results obtained by the proposed controller is better than the FOBSMC [22]. From the Figs. 12, 13, and 15 we can observe more advantages in the proposed control scheme, in the sense that it has better transient response.

4.4. Comparison with another nonlinear controller

The proposed controller was compared with the integral backstepping sliding mode control proposed in [36]. Both controllers were used on a quadrotor subjected to random disturbances. The performance responses of both controllers are shown in Fig. 5. Comparing the proposed controller to [36] in Fig. 5, it is clear that the proposed controller performs marginally better in terms of position response. The proposed control method performs better in terms of rejection disturbances. However, the tracking results of FOBSMC and IBSMC approaches are depicted in 12 to 17. As can be observed the used control methods as comparison are not effective disturbance compensation, and fail in accomplishing trajectory-tracking, especially in the first-period flight. Therefore, using the proposed controller the tracking performance in the QUAS system is enhanced in the presence of disturbances compared to existing control techniques for the QUAS system.

4.5. Quantitative analysis of the controllers

The integral of the square value of the error (ISE) $\int_{t_i}^{t_f} e^2 dt$ is used for quantitative comparison. The ISE is a numerical representation of tracking-error performance. The ISE performance of three controllers for scenarios 1 and 2 is shown respectively in Table 3 and 4. In comparison to FOBSMC and IBSMC, the proposed control scheme shows that the ISE indices are less important. The suggested control gives lower ISE error values in terms of both position and orientation of the quadrotor, as shown by the quantitative analysis in Tables 3 and 4.

Table 3: Indices de performance ISE of the scenario 1

Variable	Proposed method	FOBSMC	IBSMC
$x(t)$	0.0474	0.7673	0.2437
$y(t)$	0.0355	0.2687	0.1474
$z(t)$	0.02	0.1718	0.0491
$\psi(t)$	0.0028	0.0031	34.85

Table 4: Indices de performance ISE of the scenario 2

Variable	Proposed method	FOBSMC	IBSMC
$x(t)$	0.0534	0.1068	0.0783
$y(t)$	0.0004	0.00066	0.0007
$z(t)$	7.5 e-5	0.0003	0.0006
$\psi(t)$	0.0028	0.0029	0.0041

In comparison to the results of the other approaches, the ISE values for the tracking errors are lower. All of these findings show that the proposed control method achieves better tracking performance, including high precision tracking, quick response, smooth control commands, and high robustness.

The control approach presented in this study has higher tracking control

performance, which has been proven. It outperforms FOBSMC and IBSMC methods in terms of tracking accuracy, convergence rate, and robustness against time-varying/random disturbances.

On the other hand, for all control signals in three control strategies, the integral absolute derivative control signal (IADU) index [30] has been computed. This performance index is ideal for determining the smoothness of control signals. The HFTFSMC method creates smoother input control signals than the other strategy, as shown in Table 5, highlighting the suggested HFTFSMC structure's quality and viability. Table 5 shows the outcomes of the simulation. The proposed control method for all control signals improves smoothness, as can be demonstrated. Table 5 shows that, when compared to FOBSMC and IBSMC

Table 5: IADU index performance analysis of the scenario 2

Control signals	Proposed method	FOBSMC	IBSMC
Total torques	0.0257	0.0772	0.0438
Total thrust	19.9	20.9	20.16

methods, the proposed control can guarantees the least amount of transmission data controller-to-motor ends, significantly reducing consumption energy then reducing unnecessary costs. Another key characteristic of the proposed hybrid control is the ability to achieve convergence in a finite time. In fact, this feature has a significant benefit over other algorithms since it forces the system states to zero at a finite time, the value of which can be pre-assigned by the user based on the tun requirements.

4.6. Simulations of the proposed controller and the controller designed [36] using the same conditions

To further evaluate the performance of the controller presented in [36] and the proposed control strategy, another simulation is presented in this part. In this simulation, we use the same test set including the initial conditions and

the parameters of the quadrotor. Also, the same disturbances proposed in the paper [36] are used in the simulation. The quadrotor parameters are given as [36] :

$\mathbf{m} = 0.25kg, \mathbf{I} = diag[2.35, 2.35, 52.6]10^{-3}kg.m^2, g = 9.81m/s^2, \hbar_b = 6.1310^{-5}Ns^2,$ $\hbar_c = 2.510^{-6}Nms^2$ and $d = 0.2m$. The perturbations are selected to refer [36] :

$$\mathcal{D}_{x,y,z}(t) = \begin{cases} 0.25 + 0.01\sin(t) \quad m/s^2 \quad t \in [50, 60] \\ 0 \quad m/s^2 \\ 0.01 + 0.005\sin(t) \quad m/s^2 \quad t \in [90, 120] \end{cases}$$

$$\mathcal{D}_{\phi,\theta,\psi}(t) = \begin{cases} 0.25 + 0.01\sin(t) \quad rad.s^{-2} \quad t \in [50, 60] \\ 0 \quad rad.s^{-2} \\ 0.01 + 0.005\sin(t) \quad rad.s^{-2} \quad t \in [90, 120] \end{cases} \tag{56}$$

The results of this case are shown in Figs. 18 and 19, it is demonstrated that the suggested finite-time controller has a greater tracking accuracy than the conventional including IBSMC while starting the maneuvering flight, i.e. the take-off and landing phase. The provided control approach has a higher tracking efficacy than others, as can be shown in the results.

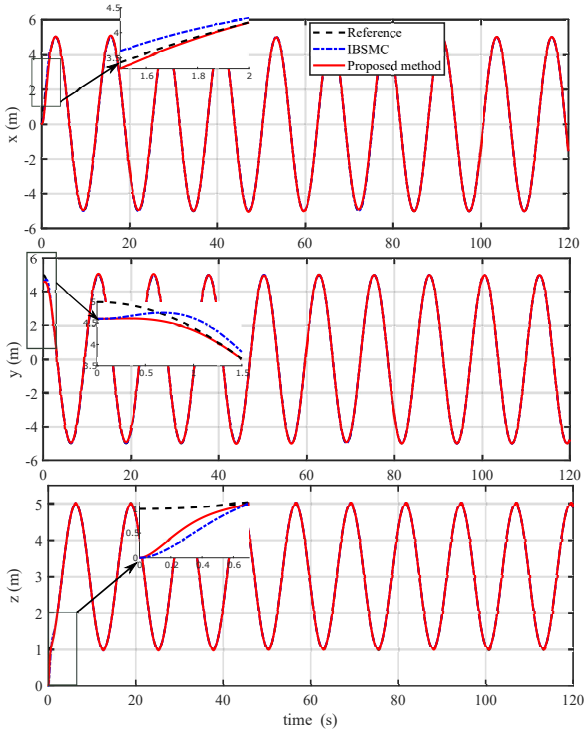

Figure 18: Position trajectory tracking performance comparison with [36] control method.

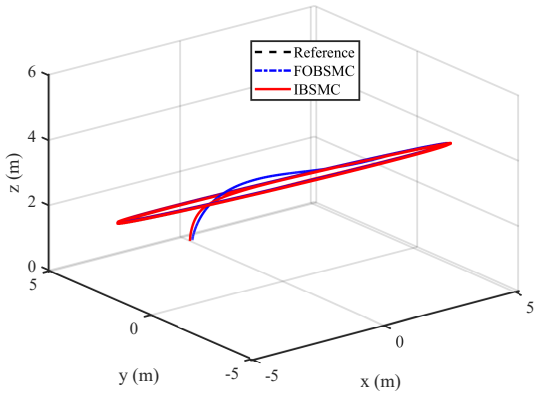

Figure 19: 3D trajectory tracking performance comparison with [36] control method.

We offer cumulative energy consumption E_M of two control torques specified by $E_M = \int_0^t |M| d\tau$ [36] in order to show the result more persuasively. The

energy consumption displayed in Fig. 20 is also good since the oscillation periods of the control torques of the provided control technique are fewer than the IBSMC method.

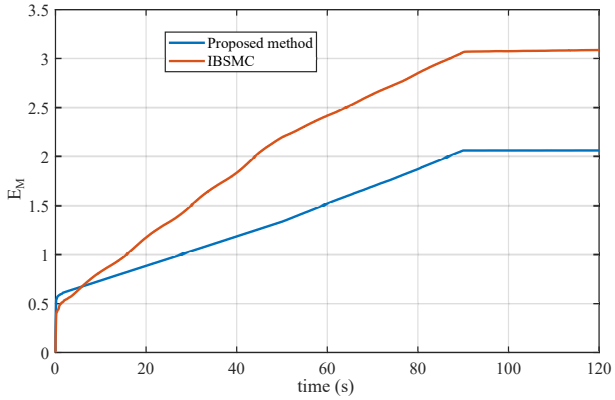

Figure 20: Energy consumption of two controllers.

4.7. Simulations of the proposed controller and the controller designed [22] using the same conditions

A four simulation collection has been carried out of the proposed controller and controller presented in [22] with the same conditions like quadrotor parameters, condition initials, and disturbances. The quadrotor parameters refer to [22] are : $\mathbf{m} = 0.53kg$, $\mathbf{I} = diag[6.28, 6.28, 6.28]10^{-3}kg.m^2$, $g = 9.81m/s^2$, $\hbar_b = 3.1310^{-5}Ns^2$, $\hbar_c = 7.510^{-7}Nms^2$ and $d = 0.232m$. The random disturbances used in this simulation are plotted in Fig. 21, which have the same amplitude and white noise as given in [22].

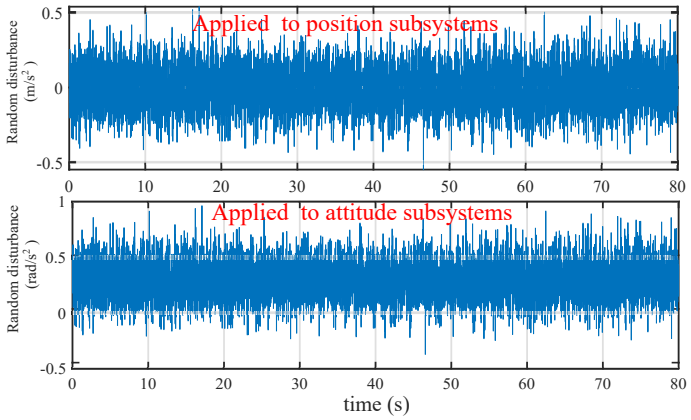

Figure 21: Gaussian random disturbances.

Figures 22 and 23 show the tracking results for rectangular trajectory tracking under Gaussian random disturbances. The simulation results show that even in the presence of wind fields, the system can track the reference trajectory. The system can fast converge and stay stable, as seen in Figures 22 and 23. The simulation's aim is to move the quadrotor quickly and with random disturbances by a square trajectory. The simulation begins with the quadrotor hovering using the same conditions for both the proposed controller and the technique proposed in [22]. The origin of the three-dimensional space above the ground is where the quadrotor is placed. As result, the proposed controller provided fast responses against random disturbances compared to the controller proposed in [22].

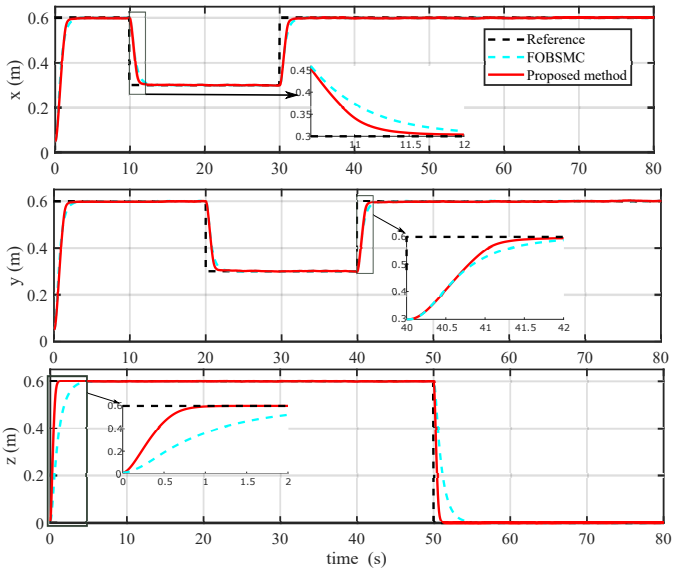

Figure 22: Position trajectory tracking performance comparison with [22] control method.

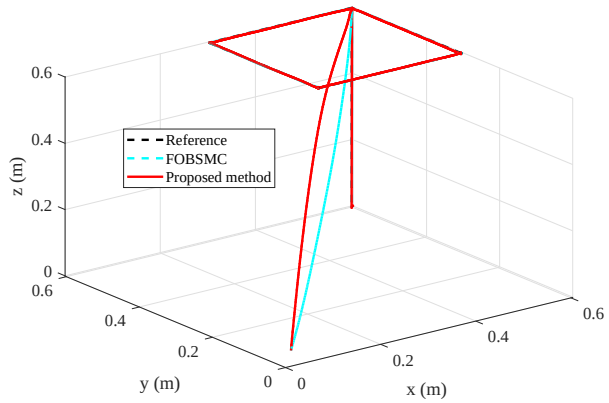

Figure 23: 3D trajectory tracking performance comparison with [22] control method.

5. Conclusions

In this paper, a trajectory-tracking control for the QUAS under external disturbances and uncertainties is presented based on the hybrid fractional-order finite-time control. The control law of the position subsystem is yielded from FO backstepping fast terminal SMC algorithm designed in this study. To succeed in

path following, the orientation control induces a flexible controller FOFTSMC deployed in this research that reject the unknown perturbation/uncertainty, inducing the finite-time stability. The proposed sliding manifold for the attitude subsystem reduces the effect of the chattering during the control phase. The concept of the suggested controllers is based on the Lyapunov stability theory which verifies and ensures the stability of the system under external disturbances. The advantages of the proposed HFOFTC are highlighted by a comparison study using simulation results. The proposed FOHFTC law has a higher performance in suppressing disturbances and gaining a lower stabilization time than the other control laws, as shown by the performance indices in the tables 3, 4, and 5.

Acknowledgement

The first author would like to thank Editor, Associate Editor, and the anonymous reviewers and Dr. Michael Defoort for their much time and constructive comments to review and improve this paper.

References

[1] D. Cabecinhas, R. Naldi, C. Silvestre, R. Cunha, L. Marconi, Robust Landing and Sliding Maneuver Hybrid Controller for a Quadrotor Vehicle, IEEE Trans. Control Syst. Technol. 24 (2016) 400412. https://doi.org/10.1109/TCST.2015.2454445.

[2] A.L. Silva, D.A. Santos, Fast Nonsingular Terminal Sliding Mode Flight Control for Multirotor Aerial Vehicles, IEEE Trans. Aerosp. Electron. Syst. 56 (2020) 42884299. https://doi.org/10.1109/TAES.2020.2988836.

[3] M. Labbadi, M. Cherkaoui, Robust adaptive nonsingular fast terminal sliding-mode tracking control for an uncertain quadrotor UAV subjected to disturbances, ISA Trans. 99 (2020) 290304. https://doi.org/10.1016/j.isatra.2019.10.012.

[4] M. Labbadi, M. Cherkaoui, Robust adaptive backstepping fast terminal sliding mode controller for uncertain quadrotor UAV, Aerosp. Sci. Technol. 93 (2019) 105306. https://doi.org/10.1016/j.ast.2019.105306.

[5] M.E. Guerrero-Sánchez, R. Lozano, P. Castillo, O. Hernández-González, C.D. García-Beltrán, G. Valencia-Palomo, Nonlinear control strategies for a UAV carrying a load with swing attenuation, Appl. Math. Model. 91 (2021) 709722. https://doi.org/10.1016/j.apm.2020.09.027.

[6] S. Harshavarthini, R. Sakthivel, C.K. Ahn, Finite-time reliable attitude tracking control design for nonlinear quadrotor model with actuator faults, Nonlinear Dyn. 96 (2019) 26812692. https://doi.org/10.1007/s11071-019-04952-4.

[7] T. Jiang, J. Huang, B. Li, Composite adaptive finite-time control for quadrotors via prescribed performance, J. Franklin Inst. 357 (2020) 58785901. https://doi.org/10.1016/j.jfranklin.2020.03.021.

[8] T. Jiang, D. Lin, T. Song, Finite-time control for small-scale unmanned helicopter with disturbances, Nonlinear Dyn. (2019). https://doi.org/10.1007/s11071-019-04882-1.

[9] X. Shao, W. Zhang, W. Zhang, Improved prescribed performance anti-disturbance control for quadrotors, Appl. Math. Model. 97 (2021) 501521. https://doi.org/10.1016/j.apm.2021.04.010.

[10] C. Hua, J. Chen, X. Guan, Adaptive prescribed performance control of QUAVs with unknown time-varying payload and wind gust disturbance, J. Franklin Inst. 355 (2018) 63236338. https://doi.org/10.1016/j.jfranklin.2018.05.062.

[11] T. Jiang, J. Huang, B. Li, Composite adaptive finite-time control for quadrotors via prescribed performance, J. Franklin Inst. 357 (2020) 58785901. https://doi.org/10.1016/j.jfranklin.2020.03.021.

[12] J. Yoo, D. Jang, H.J. Kim, K.H. Johansson, Hybrid Reinforcement Learning Control for a Micro Quadrotor Flight, IEEE Control Syst. Lett. 5 (2021) 505510. https://doi.org/10.1109/LCSYS.2020.3001663.

[13] X. Shao, X. Yue, J. Li, Event-triggered robust control for quadrotors with preassigned time performance constraints, Appl. Math. Comput. 392 (2021). https://doi.org/10.1016/j.amc.2020.125667.

[14] Yuhua Qi, Yang Zhu, J. Wang, J. Shan, H.H.-T. Liu, MUDE-based Control of Quadrotor for Accurate Attitude Tracking, Control Eng. Pract. 108 (2020) 1-24 (under review). https://doi.org/10.1016/j.conengprac.2020.104721.

[15] M. Shirzadeh, A. Amirkhani, N. Tork, H. Taghavifar, Trajectory tracking of a quadrotor using a robust adaptive type-2 fuzzy neural controller optimized by cuckoo algorithm, ISA Trans. (2020). https://doi.org/10.1016/j.isatra.2020.12.047.

[16] G. Sun, L. Wu, Z. Kuang, Z. Ma, J. Liu, Practical tracking control of linear motor via fractional-order sliding mode, Automatica. 94 (2018) 221235. https://doi.org/10.1016/j.automatica.2018.02.011.

[17] A. J. Muõz-Vázquez, V. Parra-Vega, A. Sánchez-Orta, and G. Romero-Galván, Fractional $PD - I^{\lambda}D^{\mu}$ error manifolds for robust tracking control of robotic manipulators, J. Dyn. Syst. Meas. Control. Trans. ASME, vol. 141, no. 3, 2019.

[18] Y. Wang, L. Gu, Y. Xu, X. Cao, Practical Tracking Control of Robot Manipulators with Continuous Fractional-Order Nonsingular Terminal Sliding Mode, IEEE Trans. Ind. Electron. 63 (2016) 61946204. https://doi.org/10.1109/TIE.2016.2569454.

[19] Y. Guo, B. Ma, L. Chen, R. Wu, Adaptive sliding mode control for a class of Caputo type fractional-order interval systems with perturbation,

IET Control Theory Appl. 11 (2017) 5765. https://doi.org/10.1049/iet-cta.2016.1076.

[20] A. J. Muõz-Vázquez, V. Parra-Vega, and A. Sánchez-Orta, Continuous fractional sliding mode-like control for exact rejection of non-differentiable Hölder disturbances, IMA J. Math. Control Inf. 34 (2017) 597610. https://doi.org/10.1093/imamci/dnv064.

[21] F. Oliva-Palomo, A. J. Muõz-Vázquez, V. Parra-Vega, V. Parra-Vega, C. Izaguirre-Espinosa, P. Castillo, A Fractional Nonlinear PI-structure Control for Robust Attitude Tracking of Quadrotors, IEEE Trans. Aerosp. Electron. Syst. 9251 (2019) 110. https://doi.org/10.1109/TAES.2019.2893817.

[22] X. Shi, Y. Cheng, C. Yin, S. Dadras, X. Huang, Design of Fractional-Order Backstepping Sliding Mode Control for Quadrotor UAV, Asian J. Control. 21 (2019) 156171. https://doi.org/10.1002/asjc.1946.

[23] C. Hua, J. Chen, X. Guan, Fractional-order sliding mode control of uncertain QUAVs with time-varying state constraints, Nonlinear Dyn. (2018). https://doi.org/10.1007/s11071-018-4632-0.

[24] Y. Guo, B.L. Ma, Global sliding mode with fractional operators and application to control robot manipulators, Int. J. Control. 92 (2019) 14971510. https://doi.org/10.1080/00207179.2017.1398417.

[25] C. Yin, Y. Chen, S.M. Zhong, Fractional-order sliding mode based extremum seeking control of a class of nonlinear systems, Automatica. 50 (2014) 31733181. https://doi.org/10.1016/j.automatica.2014.10.027.

[26] S. D. Mitrinovic and P. M. Vasic. Analytic inequalities. (1970) Berlin: Springer-verlag.

[27] M. Pouzesh, S. Mobayen, Event-triggered fractional-order sliding mode control technique for stabilization of disturbed quadrotor unmanned aerial vehicles, Aerosp. Sci. Technol. 121 (2022) 107337. https://doi.org/10.1016/j.ast.2022.107337.

[28] M. Labbadi, Y. Boukal, M. Cherkaoui, M. Djemai, Fractional-order global sliding mode controller for an uncertain quadrotor UAVs subjected to external disturbances, J. Franklin Inst. 358 (2021) 48224847. https://doi.org/10.1016/j.jfranklin.2021.04.032.

[29] S. Li, Y. Wang, J. Tan, Adaptive and robust control of quadrotor aircrafts with input saturation, Nonlinear Dyn. 89 (2017) 255265. https://doi.org/10.1007/s11071-017-3451-z.

[30] G. V Raffo, M.G. Ortega, F.R. Rubio, Automatica An integral predictive / nonlinear H_∞ control structure for a, Automatica. 46 (2010) 2939. https://doi.org/10.1016/j.automatica.2009.10.018.

[31] F.P. Freire, N.A. Martins, F. Splendor, A Simple Optimization Method for Tuning the Gains of PID Controllers for the Autopilot of Cessna 182 Aircraft Using Model-in-the-Loop Platform, J. Control. Autom. Electr. Syst. 29 (2018) 441450. https://doi.org/10.1007/s40313-018-0391-x.

[32] A. Oustaloup, La Commande CRONE. Paris: Hermes, 1991.

[33] B. M. Vinagre, I. Podlubny, A. Hernandez, and V. Feliu, Some Approximations of Fractional Order Operators used in Control Theory and Applications. Fractional Calculus & Applied Analysis, 2000, vol. 3, ch. 3, pp. 231248.

[34] A. Oustaloup, La Derivation Non Entiere: Synthese et Applications . Paris: Hermes, 1995.

[35] R. Malti, P. Melchior, P. Lanusse, and A. Oustaloup, Object-oriented crone toolbox for fractional differential signal processing, Signal, Image and Video Processing, vol. 6, no. 3, pp. 393-400, 2012.

[36] Z. Jia, J. Yu, Y. Mei, Y. Chen, Y. Shen, X. Ai, Integral backstepping sliding mode control for quadrotor helicopter under exter-

nal uncertain disturbances, Aerosp. Sci. Technol. 68 (2017) 299307. doi:10.1016/j.ast.2017.05.022.